SAE TECHNICAL PAPER SERIES

2000-01-2100

Analysis of Aerobatic Flight Safety Using Autonomous Modeling and Simulation

Ivan Y. Burdun
Georgia Institute of Technology

Oleg M. Parfentyev
Siberian Aeronautical Research Institute

Reprinted From: Proceedings of the 2000 Advances in Aviation Safety Conference (P-355)

SAE The Engineering Society For Advancing Mobility Land Sea Air and Space® INTERNATIONAL

Advances in Aviation Safety Conference and Exposition
Daytona Beach, Florida
April 11-13, 2000

400 Commonwealth Drive, Warrendale, PA 15096-0001 U.S.A. Tel: (724) 776-4841 Fax: (724) 776-5760

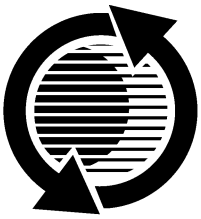

ISSN 0148-7191

Printed in USA

2000-01-2100

Analysis of Aerobatic Flight Safety Using Autonomous Modeling and Simulation

Ivan Y. Burdun
Georgia Institute of Technology

Oleg M. Parfentyev
Siberian Aeronautical Research Institute

ABSTRACT

An affordable technique is proposed for fast quantitative analysis of aerobatics and other complex flight domains of highly maneuverable aircraft. A generalized autonomous situational model of the "pilot (automaton) – vehicle – operational environment" system is employed as a "virtual test article". Using this technique, a systematic knowledge of the system behavior in aerobatic flight can be generated on a computer, much faster than real time. This information can be analyzed via a set of knowledge mapping formats using a 3-D graphics visualization tool. Piloting and programming skills are not required in this process. Possible applications include: aircraft design and education, applied aerodynamics, flight control systems design, planning and rehearsal of flight test and display programs, investigation of aerobatics-related flight accidents and incidents, physics-based pilot training, research into new maneuvers, autonomous flight, and onboard AI.

INTRODUCTION

PROBLEM – Aerobatic flight is one of the most spectacular air display events, a perfect example of coherent man-machine interaction. Aerobatics is a synthesis of the capabilities of a highly maneuverable flying machine and an experienced human pilot (**Fig. 1**). Display flights of advanced aircraft invariably attract thousands of people to major national and international air shows every year [1]. The problem of aerobatic flight safety, however, remains unresolved. There have been several aerobatics-related flight incidents and incidents with new and old aircraft types recently and in the past.

Advances in high-angle-of-attack, low-speed aerodynamics, adaptive flight control and thrust vectoring [2-5] have opened a new era in aerobatic flying. In 1989 Victor Pougatchev, a Russian test pilot flying a Sukhoj-27 fighter, had demonstrated a spectacular Cobra maneuver, first achieving in horizontal flight pitch angles exceeding 80°-110° ("Pougatchev Cobra") [2]. Cobra and other unique aerobatic figures performed to date represent an emerging class of new flight maneuvers, which will drastically expand the operational domain of next generation aircraft.

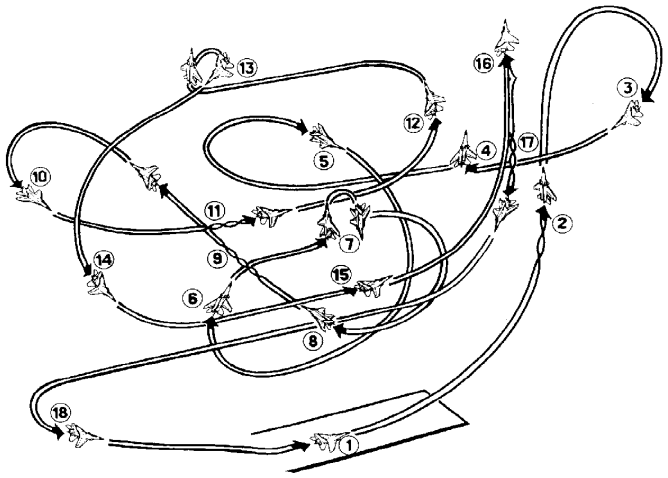

Fig. 1. Example of an aerobatic display sequence for a highly maneuverable aircraft

At the same time, these new technologies increase the likelihood of flight accidents with highly maneuverable aircraft. One of the main reasons is the limitations and shortcomings of a human pilot's knowledge, decision-making and physical capabilities revealed under extreme conditions of aerobatics. A demand is growing for new research methods and tools, which could help enhance the processes of design, test, pilot training, accident analysis and prevention, and flight control of highly maneuverable aircraft. Flight test and manned simulation have limitations when a detailed, systematic examination of a complex flight domain, such as aerobatic maneuvering, is essential [6]. More affordable and faster methods are therefore needed for this purpose. Thus, the *problem* under study is formulated as follows: (1) techniques for fast, inexpensive and efficient analysis of aerobatic flight,

and (2) virtual test and evaluation of aerobatic flight performance of a highly maneuverable aircraft using these techniques.

The following factors may compromise aerobatic flight safety: a highly dynamic 4-D maneuvering environment, performance of flight and control at and beyond the edge of the vehicle's normal operational envelope, ground proximity, extreme physical and mental workload experienced by the pilot, last-minute changes made to a preplanned display scenario, lack of pilot's or designer's knowledge of the vehicle behavior in non-standard (multi-factor) situations, and unforeseen obstacles (birds, other aircraft, etc.). Negative effects of these factors, including the potential for "chain reaction" – a spontaneous, irreversible transition of a safe flight towards a catastrophe [7], must and can be examined in advance.

SOLUTION APPROACH – One possible solution approach to this problem, called *autonomous situational modeling and simulation of flight*, is introduced below. A hypothetical yet realistic aerobatic flight scenario is employed to demonstrate this technique. It is based on two concepts: an AI situational pilot model and a flight situation scenario [8, 9]. The words "autonomous" and "situational" mean that a human pilot's decision-making mechanism and the content of aerobatic flight situations (maneuvers) are modeled mathematically, together with the vehicle flight dynamics. This enables flexible planning, fast-time execution, and, if necessary, multiple repetitions (in exact detail or modified) of various aerobatic sequences on a PC. Piloting and programming skills are not required in this process.

OBJECTIVE – The *subject* of this study is identification of complex cause-and-effect relationships in the "pilot (automaton) – vehicle – operational environment" system behavior under aerobatic flight conditions. Another research focus is new graphic formats for mapping knowledge of a complex flight domain in simulation. The *overall objective* is to demonstrate the capabilities of the autonomous modeling and simulation technique as a virtual flight test and evaluation tool. This technique is intended for use in the design, test and operational phases of the vehicle's life cycle.

DISCLAIMER – In this paper, a generalized model of an advanced aerobatic aircraft is employed as a virtual test article. This model does not represent any particular aircraft type. Input characteristics and design parameters of this notional vehicle are compiled from several published sources. Some (missing) characteristics are entirely hypothetical. A proprietary flight modeling and simulation software tool called VATES is used in this study.

The examined flight scenario does not represent or reconstruct any actual flight display sequence or accident. It has been designed solely to demonstrate the developed technique and its capabilities in studying complex aerobatic maneuvers. This paper does not contain vehicle- or case-specific piloting instructions or flight safety recommendations for immediate use. Some notations and concepts, used or introduced in this study, may differ from related national standards.

PAPER STRUCTURE – The paper includes the following main sections: a brief description of the employed virtual test article; a description of the employed aerobatic scenario (example); results of aerobatic modeling and simulation, including examples of identified unsafe and hypothetical maneuvers; a brief discussion of results; conclusions. Several supplementary tabular and graphic materials are located in Appendix.

VIRTUAL FLIGHT TEST ARTICLE

AIRCRAFT TYPE – In this study, the *virtual test article* under study is a mathematical model of a highly maneuverable notional jet fighter or trainer, which summarizes key features of modern highly maneuverable aircraft. In particular, the model has advanced low-speed aerodynamics, which permits operational use of high angles of attack and pitch (up to 90°-135°). The "aircraft" is equipped with two engines, providing a maximum thrust-to-weight ratio of about 1.15-1.3 (at SL). It also has a 2-D thrust vectoring capability for flight path and attitude control at low and medium speeds.

FLIGHT CONTROLS – The vehicle's primary flight controls include canards coupled with elevator, ailerons, rudder, throttles, and 2-D thrust vectoring nozzles. The model's secondary control devices are: flaps coupled with slats, interceptors, airbrakes, undercarriage control (extended, interim, and retracted positions), thrust reversers, and main wheel brakes.

DESIGN PARAMETERS – Selected design parameters of the model are shown in **Table 1**.

Table 1. Design parameters of the virtual test article

Parameter	Value	Unit
Aileron deflection range	[-25; 20]	°
Aircraft C.G. travel (along *X* axis)	[12; 30]	%
Aircraft empty mass	14000.0	kg
Aircraft takeoff mass	20000.0	kg
Elevator/canards deflection range	[-25; 25]	°
Engine TV range (*XY* plane)	[-30; 30]	°
Engine TV range (*XZ* plane)	[-30; 30]	°
Flap deflection range	[0; 40]	°
Fuel mass	2000.0	kg
Interceptors/airbrake deflection range	[0; 50]	°
Mean aerodynamic chord	3.197	m
Number of engines	2	-
Number of model's input characteristics	155	-
Payload	4000.0	kg
Rudder deflection range	[-25; 25]	°
Throttles travel range	[-50; 70]	%
Thrust-to-weight ratio (at SL)	1.15-1.3	-
Wheel brakes on-off control switch	[0; 1]	-
Wheels on-off control switch	[0; 1]	-

AUTONOMOUS SITUATIONAL MODEL

The *autonomous situational model of flight* employed in this study is a set of interconnected generalized mathematical models, which model a human pilot's situational (tactical) decision-making mechanism, a pre-defined flight scenario, vehicle flight dynamics, and a given subset of operational conditions [6-11]. This model has been implemented using a proprietary software tool called VATES.

PILOT MODEL – A human pilot's decision-making mechanism is represented by a discrete-continuous situational model [8]. The main assumption of this model is that at the situational level of decision making a human pilot uses basic knowledge objects of two types: the *event* $\mathbf{E}_i$ (a *discrete component*) and the *process* $\mathbf{\Pi}_j$ (a *continuous component*). The following *attributes* of a pilot's situational decision making mechanism are modeled: a vector of observed system state variables for each control variable of a piloting process called piloting task, pilot errors, response delays, interim goal states, insensitivity of system state observations, frequency of state observations and control increments, feedback gains, and some other. More detailed explanation can be found in [8, 10].

FLIGHT SITUATION MODEL – The triple ($\mathbf{E}_i$, $\mathbf{\Pi}_j$, $\mathbf{E}_k$) represents an *elementary flight situation*, where the *source event* $\mathbf{E}_i$ opens the process $\mathbf{\Pi}_j$ in simulation and the *target event* $\mathbf{E}_k$ closes it. A subset of *flight control processes* is represented by objects of the following three types:

- *"piloting task"* **T** - a continuous flight control process with feedback)
- *"system state observer"* **O** - a process of providing feedback on the current system state to **T**, and
- *"control procedure"* **P –** a singular action with controls without a continuous feedback.

A set of all the events planned or expected to appear in some flight is called the *calendar of flight events*, $\mathbf{\Omega}(\mathbf{E})$. A united list of all continuous components of **S** is called the *calendar of flight processes*, $\mathbf{\Omega}(\mathbf{\Pi})$.

FLIGHT SCENARIO – The *[aerobatic] flight situation scenario*, **S**, is a plan for implementing required flight sequence and the associated piloting tactics in a simulation experiment. It is depicted as a directed graph, $\mathbf{S} = \mathbf{\Omega}(\mathbf{E}) \cup \mathbf{\Omega}(\mathbf{\Pi})$. In this graph, vertices or events $\mathbf{\Omega}(\mathbf{E})$ and arcs or processes $\mathbf{\Omega}(\mathbf{\Pi})$ are linked together, forming a logical framework of an aerobatic flight situation under study. Note that a scenario graph may be viewed as union of its elementary flight situations. This simple yet realistic event-process formalization helps capture cause-and-effect and other key relationships of a complex flight situation, thus mapping its invariant logical structure. A flight scenario can be mapped into a set of input data files for autonomous simulation. Scenarios can be easily modified to generate a subset of "neighboring" flight situations in *"what-if" flight simulation experiments*. These derivative cases may stand for variations in the original aerobatic scenario, e.g.: in piloting tactics and interim goals, pilot errors, mechanical failures, and weather conditions.

FLIGHT DYNAMICS MODEL – The vehicle 6-DOF motion is described by a system of first-order ordinary differential equations with non-linear right parts, in the form of quaternions. Thus, the majority of complex aerobatic maneuvers can be simulated without restricting the vehicle pitch, roll and yaw (no discontinuity occurs in attitude calculations at $k\pi/2$ and $k\pi$ points). The flight dynamics model is implemented in the form of a generalized flight simulation software complex explained below. Thus, no software re-programming is needed, if the vehicle's definition or a flight scenario is to be modified, because these two components are fully independent of the generalized flight modeling algorithms and programs.

INPUT REQUIREMENTS – A pre-requisite for successful application of the model is the availability of a comprehensive vehicle's definition in the form of a database of calculated or/and experimental *input characteristics*: geometry (MAC, wing gross area, C.G., etc.); static aerodynamic characteristics; stability and control derivatives; moments and products of inertia; engine characteristics, including reversed thrust; parameters of actuators and automatic control system if any; ground effects and other weather conditions if present; landing gear characteristics (shocks, wheels, brakes, control); aeroelasticity effects.

In this study, the notional vehicle's input database incorporates over 150 aerodynamic and other characteristics. These characteristics are presented as functions of 1-3 flight variables (arguments), and coded as look-up tables. The total number and average dimensionality of input characteristics of a flight model may be used to measure the *level of comprehensiveness* of the model. (Note: in practical applications, results of flight modeling and simulation are likely to be valid, if the minimal number of model's input characteristics is 30-50 and the average dimensionality of these functions is equal or higher than 2.)

FLIGHT SIMULATION SOFTWARE – The *Virtual Autonomous Test and Evaluation Simulator* (VATES) is used to model and simulate the "pilot (automaton) – vehicle – operational environment" system dynamics in aerobatic flight. VATES consists of two parts: a generalized complex for flight modeling and simulation and data processing and a database of virtual flight experiment scenarios.

The first part includes: specifications, algorithms, a library of FORTRAN modules, which model vehicle flight dynamics, human piloting, flight scenario and perform other simulation and processing functions according to a given experimentation plan. The second part is a database, which contains a "vehicle's definition" (constant

parameters and flight regime dependent input characteristics) and a library of virtual flight experiment scenarios. A *virtual flight experiment [test] scenario* consists of the four groups of data files: experiment control parameters, vehicle's definition, flight situation scenario, and output specification parameters. It is loaded before each experiment. Note that a flight control scenario is a subset of a flight situation scenario, which is a subset of a virtual flight experiment scenario.

The distinguishing features of VATES include (**Table A1**): mapping of complex flight domains into concise and clear scenarios for modeling; integration of a human pilot's tactics and operational factors via invariant cause-and-effect links; easy planning and execution of virtual flight test cases on a computer by a non-pilot and non-programmer; simulation of flight much faster than real time; simulation of pilot's actions on a computer; compact retention of flight scenarios for future reuse; easy repetition and modification of flight scenarios.

The authors' experience of studying complex flight domains using this tool for over 15 years includes 16 flying aircraft types and six design projects and more than 350 types of flight scenarios. This experience has demonstrated that the flight scenario concept allows to plan and simulate on a computer the majority of complex flight cases (actual, hypothetical, and mixed ones) under various operational conditions for any vehicle, if the vehicle's aerodynamic and other input characteristics essential for the flight regimes of interest are available.

EXAMINED AEROBATIC SCENARIO

ASSUMPTIONS – A real aerobatic flight sequence of a highly maneuverable aircraft is depicted in **Fig. 1**. Structure of this scenario is clear from the diagram. More detail on this display flight and its background can be found in [1]. In the presented study, a hypothetical aerobatic flight scenario **S** of the notional vehicle described above has been developed and virtually tested instead. This is mainly because we use a notional, not real test article. Nevertheless, this hypothetical scenario repeats almost all the figures from **Fig. 1**. In addition, several new aerobatic elements have been included into **S**.

PHASES OF FLIGHT – Aerobatic flight scenario design is a creative, difficult-to-formalize process. It depends on many factors, such as flight purpose, location, and duration, vehicle performance, and other. In this study, the examined aerobatic scenario is presented as a sequence of the following ten *phases*, $P_{(1)}$, …, $P_{(10)}$:

- Takeoff, vertical climb, 180° right roll, and ¾ loop
- First Pougatchev Cobra maneuver
- Left turn, 270° heading change, and ¼ loop
- Vertical climb and vertical descent with multiple rolls
- Loop, vertical climb; descent from a fixed 90° pitch vertical position
- Right turn for heading reversal, second Cobra maneuver
- Loop with 90° roll, followed by a loop with a single Somersault and descent at a medium pitch angle
- Vertical climb, sharp dive using TVC, double Somersault, and tail-down slide
- S-turn to gain the runway heading (0°)
- Landing approach, landing, touchdown, and groundroll.

FLIGHT SEGMENTS – On the next level of a top-down analysis of this scenario, more refined components of flight, called segments, are identified. The *flight segment*, *S*, is formalized as some characteristic flight situation, which has pre-defined (constant or varying) interim goal states, measured by a subset of relevant observed system state variables, and a subset of flight events and flight control processes. Usually, a flight segment represents an aerobatic maneuver or some frequently used sequence (concatenation) of maneuvers.

All segments constituting flight phases $P_{(1)}$, …, $P_{(10)}$ are specified in **Table 2**. Each segment $S_{k\text{-}l}$ is coded by a pair of sequential numbers, *k*-*l*, from 1-2 to 31-32, which indicates, respectively, the start point and the end point of this segment within a display sequence or phase $P_{(i)}$. Thus, the total number of segments in this scenario is equal to 31. The last two columns in **Table 2** contain codes $i(\mathbf{E}_*)$ and $i(\mathbf{E}^*)$ of the boundary events, $\mathbf{E}_*$ and $\mathbf{E}^*$, of segments $S_{k\text{-}l}$; where $\mathbf{E} \in \Omega(\mathbf{E})$ and $S_{k\text{-}l} \in \{S_{1\text{-}2}, \ldots, S_{31\text{-}32}\}$. That is, event $\mathbf{E}_*$ begins a segment, while $\mathbf{E}^*$ finishes it. Note that $i(\mathbf{E}_*)|S_{(k+1)\text{-}(l+1)} = i(\mathbf{E}^*)|S_{k\text{-}l}$, where $k = 1, \ldots, 31$ and $l = k+1$. These boundary events are represented by their codes, $i(\mathbf{E}_*)$ and $i(\mathbf{E}^*)$, and will be defined below. A compound code *m*/*n* means that the boundary between two segments is located between events $\mathbf{E}_m$ and $\mathbf{E}_n$.

Thus, this flight scenario can be split into components as follows: $\mathbf{S} = P_{(1)} \,||\, P_{(2)} \,||\, \ldots \,||\, P_{(10)}$, where $P_{(1)} = S_{1\text{-}2} \,||\, \ldots \,||\, S_{4\text{-}5}$; $P_{(2)} = S_{5\text{-}6} \,||\, S_{6\text{-}7}$; $P_{(3)} = S_{7\text{-}8} \,||\, S_{8\text{-}9}$; $P_{(4)} = S_{9\text{-}10} \,||\, \ldots \,||\, S_{13\text{-}14}$; $P_{(5)} = S_{14\text{-}15} \,||\, \ldots \,||\, S_{16\text{-}17}$; $P_{(6)} = S_{17\text{-}18} \,||\, S_{18\text{-}19}$; $P_{(7)} = S_{19\text{-}20} \,||\, \ldots \,||\, S_{22\text{-}23}$; $P_{(8)} = S_{23\text{-}24} \,||\, \ldots \,||\, S_{25\text{-}26}$; $P_{(9)} = S_{26\text{-}27} \,||\, \ldots \,||\, S_{29\text{-}30}$; and $P_{(10)} = S_{30\text{-}31} \,||\, S_{31\text{-}32}$.

Symbol || denotes the operation of concatenation in time of two neighboring components.

FLIGHT EVENTS – A calendar of the flight events, which implement scenario **S**, is defined in **Table A2**. The total number of the flight events constituting **S** is 98, $N(\Omega(\mathbf{E})) = 98$. A subset of these events, which are planned for the first phase of flight, $P_{(1)}$, is also shown in **Table 3**. For each $\mathbf{E}_i$ the following attributes are shown: time instant $t(\mathbf{E}_i)$ when $\mathbf{E}_i$ has been recognized, event's code and name. Event names look exactly as they appear in a flight scenario output listing. A generalized data structure used to specify each event $\mathbf{E}_i$ in simulation, including its recognition criterion, is described in [8, 10].

Table 2. Phases and segments of aerobatic flight scenario **S**

Code	Name	$i(E_*)$	$i(E^*)$
Phase $P_{(1)}$: *"Takeoff, vertical climb, 180° right roll, and ¾ loop"*			
1-2	Groundroll and take-off	101	109
2-3	Transition to vertical (90° pitch) climb by TVC	109	114
3-4	180° roll in vertical climb	114	124
4-5	¾ loop	124	118
Phase $P_{(2)}$: *"First Pougatchev Cobra maneuver*			
5-6	Deceleration. First Pougatchev Cobra	118	405
6-7	Post-Cobra path	405	500
Phase $P_{(3)}$: *"Left turn, 270° heading change, and ¼ loop"*			
7-8	Left turn (-65° bank) and 270° heading change	500	601
8-9	¼ loop (transition to vertical climb)	601	605
Phase $P_{(4)}$: *"Vertical climb and vertical descent with multiple rolls"*			
9-10	720° roll in vertical climb	605	606
10-11	Vertical climb at ~90° pitch	606	701
11-12	Path reversal by TVC and vertical descent (-90° pitch)	701	706
12-13	360° roll in vertical descent (~-90° pitch)	706	707
13-14	Vertical descent	707	703
Phase $P_{(5)}$: *"Loop, vertical climb; descent from a fixed 90° pitch vertical position"*			
14-15	Full loop	703	704/ 801
15-16	Energy conversion in vertical climb	704/ 801	802
16-17	Fixed vertical position (90° pitch) at low speed. Sharp change of path to descend	802	804
Phase $P_{(6)}$: *"Right turn for heading reversal, second Cobra maneuver"*			
17-18	Left turn (at -55° bank) – 180° heading change	804	805
18-19	Pre-Cobra path. Second Cobra	805	910
Phase $P_{(7)}$: *"Loop with 90° roll, followed by a loop with a single Somersault and descent at a medium pitch angle"*			
19-20	Restoration of energy, attitude, and safety balance	910	912
20-21	¼ loop with 90° roll. ¾ loop	912	914
21-22	540° (one and a half) Somersault and full loop	914	918
22-23	35° pitch descent under TVC	918	922
Phase $P_{(8)}$: *"Vertical climb, sharp dive using TVC, double Somersault, and tail-down slide"*			
23-24	Transition to a vertical climb (90° pitch)	922	945
24-25	Sharp dive from nose-up position using TVC Energy and safety balance restoration	945	947
25-26	720° (double) Somersault and tail-down (80° pitch) slide	947	950
Phase $P_{(9)}$: *"S-turn to gain the runway heading (0°)"*			
26-27	Restoration of aircraft potential energy	950	951
27-28	Gaining a small pitch angle (7°) and 70° bank for left turn	951	951/ 952
28-29	First part of S-turn (at 70° bank)	951/ 952	953
29-30	Second part of S-turn to reach runway heading	953	954
Phase $P_{(10)}$: *"Landing approach, landing, touchdown, and groundroll"*			
30-31	Descent to H_{wheels}=15 *m* at runway heading	954	956
31-32	Landing, groundroll, deceleration, and stop	956	959

Table 3. A subset of flight events $\mathbf{E}_i$ for phase $P_{(1)}$

$t(E_i)$, *s*	*i*	Name
0.1	101	"Groundroll start ..."
4.0	102	"Speed VR achieved"
4.7	103	"Nose wheel off runway"
5.5	105	"Left wheel off runway"
5.5	106	"Right wheel off runway"
6.2	107	"Lift off point"
6.5	104	"Pitch 20 deg"
7.0	108	"H to retract wheels"
7.4	110	"Pitch 30 deg
7.9	109	"Altitude 30 m
8.6	111	"Pitch 60 deg"
9.6	113	"H = 100 m"
10.6	112	"Vertical attitude
12.1	114	"Start of aileron pulse"
15.0	123	"Roll 135 deg & pitch 90"
15.8	115	"Roll 180 deg & pitch 90"
16.9	124	"Start of 3/4 loop"
22.2	116	"Max altitude (1/4 loop)"
25.4	117	"Nose down (2/4 loop)
27.3	121	"Speed exceeds 250 km/h"
33.0	118	"Nose level (3/4 loop)"

The actual timing of flight events is not known before a simulation experiment, except for ones planned explicitly by time. In an experiment each event is recognized based on its unique *recognition criterion* [10]. For example, the recognition criterion for event $\mathbf{E}_{102}$: "Speed VR achieved" (ref. **Table 3**) is: [V_{IAS} > 180 *km/h*], or using the VATES input format: [77 GT 180.0]; where $x_{77} \equiv V_{IAS}$, $x_{77} \in \Omega(\mathbf{X})$, and GT stands for a "greater than" (>) relation.

FLIGHT CONTROL PROCESSES – A list of the piloting tasks required for implementing phase $P_{(1)}$: *"Takeoff, vertical climb, and ¾ loop at 180° right roll"*, $\Omega(\mathbf{T})|P_{(1)}$, is presented in **Table 4** as an example. The source and target events of these processes are indicated by codes from **Table 3**. A set of system state observers (not shown) has also been developed for all piloting tasks from $\Omega(\mathbf{T})$. All the control procedures planned for this phase is shown in **Table 5**.

Table 4. A subset of piloting tasks $\mathbf{T}_j$ for phase $P_{(1)}$

j	E_*	E^*	Name	Control vector, *u*		
1	101	103	"Steer runway centerline"	ζ	-	-
2	104	109	"Keep pitch 30 deg in initial climb"	η	χ	ζ
3	109	111	"Keep side balance"	χ	ζ	-
4	111	114	"Keep vertical path by TV"	φ_{TV}	χ	ζ
11	114	124	"Keep pitch 85 deg by TV in roll"	φ_{TV}	ζ	-
12	123	124	"Maintain bank (w) 180 deg"	χ	-	-
5	124	118	"Keep side balance in loop"	χ	ζ	-

Table 5. A subset of control procedures $\mathbf{P}_k$ for phase $P_{(1)}$

k	$\mathbf{E}_*$	$\mathbf{E}^*$	Name	Control vector, *u*			*m*	*G*
1	102	-	"Elevator – up"	η	-	-	ABS	-12
2	108	-	"Wheels – up"	K_{LG}	-	-	ABS	0
3	109	-	'Elevator & TV – up"	φ_{TV}	η	-	REL	
5	112	-	"Elevator & TV to zero"	φ_{TV}	η	-	ABS	0
7	114	-	"Right aileron – up"	χ	-	-	ABS	-20
9	124	-	"Elevator – up to loop"	η	-	-	REL	-15
11	124	-	"Thrust to idle	δ_{ENG1}	δ_{ENG2}	-	ABS	5
12	121	-	"Airbrakes & interceptors – on"	δ_{ABR}	δ_{INT1}	δ_{INT2}	ABS	50

Note. The total number of elements in sets $\Omega(\mathbf{T})$, $\Omega(\mathbf{O})$ and $\Omega(\mathbf{P})$ are, respectively: 38, 98, and 66, i.e. $N(\Omega(\Pi)) = N(\Omega(\mathbf{T})) + N(\Omega(\mathbf{O})) + N(\Omega(\mathbf{P})) = 202$. That is, the overall number of the flight control processes, which are required to implement this 415-second flight scenario, is about 200. Index $N(\Omega(\Pi))$ together with $N(\Omega(\mathbf{E}))$ may serve as *measures of [logical] complexity of a flight scenario* and pilot's mental workload in a particular situation (phase, segment, or flight). By recording time instants of source ($\mathbf{E}_*$) and target ($\mathbf{E}^*$) events of flight processes it becomes possible to measure how this scenario unfolds in time. The parameter *m* (**Table 5**) indicates the method of defining the control goal of $\mathbf{P}_i$. If *m* = REL, then the goal value of control vector (u_1, …, u_3) is calculated as *G* plus the value of (u_1, …, u_3) when $\mathbf{P}_i$ has started. This is a method of "relative" specification of flight goals. If *m* = ABS, then the goal value of (u_1, …, u_3) is set to *G* ("absolute" specification).

INITIAL CONDITIONS – The initial conditions of flight performed according to scenario **S** are summarized in **Table 6** (ref. also **Table 1**).

SCENARIO DESCRIPTION (EXAMPLE) – A formalized scenario of phase $P_{(1)}$: *"Takeoff, vertical climb, 180° right roll, and ¾ loop"*, is explained below. In this example, the events and processes from **Tables 3-5** are used. The objective of this example is to take readers through the logic of a scenario planning process and demonstrate that the "event-process" flight specification language is clear to analysts and pilots, and it is easy to use. Similar verbal descriptions can be compiled for other phases and segments of flight. (Note: In simulation, only input files containing specification of sets $\Omega(\mathbf{E})$, $\Omega(\mathbf{T})$, $\Omega(\mathbf{O})$, and $\Omega(\mathbf{P})$ are required.)

Table 6. Initial flight conditions

i	Variable name	Value	Unit
186	Altitude (measured at main wheels' bottom)	-0.31	*m*
78	Aircraft C.G. location on MAC	20.0	*%*
250	Duration of flight	415.0	*s*
3	Elevator/canards position	5.0	*deg*
25	Flaps setting	10.0	*deg*
76	Flight path angle	0.0	*deg*
77	Indicated air speed	5.0	*km/h*
214	Joint thrust vectoring mode	1	-
44	Left gear shock absorber displacement	0.27	*m*
43	Nose gear shock absorber displacement	0.22	*m*
14	Pitch angle	0.6	*deg*
45	Right gear shock absorber displacement	0.27	*m*
251	Runway-wheels adhesion factor	0.7	-
201	Table formation step	0.25	s
63	Throttle 1 setting	60.0	%
64	Throttle 2 setting	60.0	%
89	Wheels control switch (wheels "on")	1.0	-

The first phase starts on the ground, at event $\mathbf{E}_{101}$: "Groundroll start ...". Note that $\mathbf{E}_{101}$ begins the whole flight (the initial conditions of flight summarized in **Table 6**). With this event, only one piloting task $\mathbf{T}_1$: "Steer runway centerline" is launched. To perform this task, the "silicon pilot" is requested to use rudder ζ as a control variable, $\zeta \equiv x_{10}$, and to observe a vector of three system state variables: $(\mathbf{r}`, \beta`, \beta) \equiv (x_{150}, x_{143}, x_{11},)$. This state vector is the main attribute of a feedback process accompanying $\mathbf{T}_1$ called the system state observer, $\mathbf{O}[\mathbf{T}_1]$. Another attribute of $\mathbf{O}[\mathbf{T}_1]$ is an interim flight goal required to achieve in $\mathbf{T}_1$; that is to keep the yaw angle at zero (as no wind is modeled during groundroll, we assume that $\beta \cong \psi$). After reaching the rotation airspeed V_R=180 *km/h*, event $\mathbf{E}_{102}$: "Speed VR achieved" will be recognized. At this point, the pilot will start a control procedure $\mathbf{P}_1$: "Evevator - up", using elevator to rotate the model according to the elementary situation ($\mathbf{E}_{102}$, $\mathbf{P}_1$, $\mathbf{E}^*[\mathbf{P}_1]$). Note that the target event of $\mathbf{P}_1$, $\mathbf{E}^*[\mathbf{P}_1]$, is not specified explicitly in **Table 5**. It will be recognized automatically, when elevator reaches its goal position. The latter is specified as an attribute of $\mathbf{P}_1$ in the procedure's input frame (not shown).

During the transition from groundroll to airborne the following events are to be recognized and signaled: $\mathbf{E}_{103}$: "Nose wheel off runway", which closes the groundroll piloting task $\mathbf{T}_1$ ($\mathbf{E}_{103} \equiv \mathbf{E}^*[\mathbf{T}_1]$); $\mathbf{E}_{105}$: "Left wheel off runway"; $\mathbf{E}_{106}$: "Right wheel off runway"; $\mathbf{E}_{107}$: "Lift off point". Also, when the aircraft pitch reaches about 20° (event $\mathbf{E}_{104}$: "Pitch 20 deg") the pilot will commence a new piloting task $\mathbf{T}_2$ to perform initial climb, $\mathbf{T}_2$: "Keep pitch 30 deg in initial climb". In this process, the pilot model will use elevator, ailerons and rudder (the latter two are applied

for keeping side balance). The system state observers of $\mathbf{T}_2$ are defined as follows. $\mathbf{O}[\mathbf{T}_2|\eta]$: ($\mathbf{q}^{\backprime W}$, $\mathbf{q}^W$, ϑ^W), $\mathbf{O}[\mathbf{T}_2|\chi]$: ($\mathbf{p}^{\backprime W}$, $\mathbf{p}^W$, ϕ^W), and $\mathbf{O}[\mathbf{T}_2|\zeta]$: ($\mathbf{r}^{\backprime}$, $\beta^{\backprime}$, β). The goal vector for these three subsets of control and observation processes is: (ϑ^W, ϕ^W, β) = (30°, 0°, 0°).

When the vehicle reaches an altitude of 10.7 *m* (event $\mathbf{E}_{108}$: "H to retract wheels"), a control procedure $\mathbf{P}_2$: "Wheels - up" will be launched. Event $\mathbf{E}_{110}$: "Pitch 30 deg" will indicate an interim pitch angle (this is a rudimentary event, and no action will be taken when it occurs). At event $\mathbf{E}_{109}$: "Altitude 30 m" control procedure $\mathbf{P}_3$ will start to rotate the vehicle further to a vertical climb position, by using simultaneously elevator η and vertical thrust vectoring φ_{TV}, $\mathbf{P}_3$: "Elevator & TV - up". At the same time (from $\mathbf{E}_{109}$), the pilot will also switch to a new piloting process $\mathbf{T}_3$: "Keep side balance" using ailerons and rudder. Beginning from a pitch angle of about 60° (event $\mathbf{E}_{111}$) the pilot will maintain a vertical climb path using thrust vectoring, via process $\mathbf{T}_4$: "Keep vertical path by TV".

When the vehicle is at an altitude of about 100 *m* (event $\mathbf{E}_{113}$) and its pitch attitude is close to a vertical position (event $\mathbf{E}_{112}$), elevator and thrust vectoring nozzles will be gradually returned to zero by means of $\mathbf{P}_5$: "Elevator & TV $\rightarrow$ 0". Then, at an altitude of ~250 *m* ($\mathbf{E}_{114}$) the pilot will apply a step input by ailerons to roll the vehicle clockwise (procedure $\mathbf{P}_7$), while keeping pitch about 90° for vertical climb by means of thrust vectoring and a zero sideslip angle by rudder ($\mathbf{T}_{11}$). When a 135° bank angle (ϕ^W) is achieved in roll at $\vartheta^W \approx 90°$ (this is event $\mathbf{E}_{123}$), the pilot will begin maintaining a half-roll (ϕ^W=180°) by ailerons and continue vertical climb ($\mathbf{T}_{12}$). At an altitude of about 500 *m* ($\mathbf{E}_{124}$), a ¾ loop maneuver will begin. The loop will be initiated at $\mathbf{E}_{124}$ by applying a fixed step elevator input ($\mathbf{P}_9$). During the loop, the aircraft side balance will be maintained through piloting task $\mathbf{T}_5$ by means of ailerons and rudder to keep goal state (ϕ^W, β) = (180°, 0°). At the same time (at $\mathbf{E}_{124}$), throttles will be temporarily put to idling ($\mathbf{P}_{11}$) to reduce speed. When a "12 o'clock" and then a "9 o'clock" position are reached during the loop, events $\mathbf{E}_{116}$: "Max altitude (1/4) loop" and $\mathbf{E}_{117}$: "Nose down (2/4) loop" will be indicated for information purposes. Somewhere during a descending part of the loop an excessive airspeed is expected ($\mathbf{E}_{121}$). Once the latter is true, a procedure of extending airbrakes and interceptors ($\mathbf{P}_{12}$) will be launched to decelerate the vehicle from this point. Phase $P_{(1)}$: *"Takeoff, vertical climb, 180° right roll, and ¾ loop"* ends, when the system arrives to event $\mathbf{E}_{118}$: "Nose level (3/4) loop". With this event, second phase $P_{(2)}$: *"First Pougatchev Cobra"* will begin without interruption – ref. **Table 2**.

MODELING AND SIMULATION RESULTS

OBJECTIVE – The objective of the presented series of virtual aerobatic experiments is two-fold: (1) to identify required control tactics (the parameters of the flight events and control processes constituting **S**) and reproduce this scenario in autonomous simulations, and (2) to demonstrate some possible unsafe and new maneuvers.

EXPERIMENT STATISTICS – A sequential number of a flight experiment ("flight") serves as its identification code in analysis, e.g. Flight No. 1457. The total number of "flights" conducted according to scenario **S** or its modifications is about 2000. The duration of one full aerobatic sequence, from a start point on the ground at take-off and to a stop point after landing, is 415 seconds. However, the average duration of simulated flights is 200-300 seconds. This is because there have been cases, in which the vehicle "crashed" before reaching the final event ($\mathbf{E}_{959}$) of the scenario. Experiments have also been conducted to check separate components of **S**. Thus, the *total flight time* accumulated by the "silicon pilot" (and, therefore, by the flight analyst) is approximately: 250x2000/3600 ≈ 138 hours. This number may serve as a rough estimate of the *virtual flight test experience* learned by an analyst from autonomous modeling and simulation. The overall computer time required for running one 415-second flight experiment on a 450 MHz Pentium II PC using VATES is 15-20 seconds. This includes the processor time for flight model calculations and the time of disk read-write operations. Thus, for this particular vehicle and computer model virtual flight experiments run 20-28 faster than real time.

FLIGHT VARIABLES – A virtual flight experiment is monitored and measured using a full *system state vector x* containing 350 output (flight) variables, $x = (x_1, \ldots, x_{350})$, or its subset. These variables describe various aspects of the "pilot (automaton) – vehicle – operational environment" system behavior [8, 10]. A subset of 20 *output flight variables* has been selected to record the system behavior in a simulation experiment, ref. **Table 7**. In **Table 7** the code of variable x_i is a sequential number, *i,* of this variable in the system state vector x, $x = (x_1, \ldots, x_i, \ldots, x_{350})$.

Table 7. A subset of 20 output flight variables used in analysis

Code	Name	Symbol	Unit
186	Altitude (measured at main wheels)	H_{wheels}	m
12	Bank angle	ϕ	deg
330	Bank angle (wind axes)	ϕ^W	deg
21	East coordinate	E	m
3	Elevator/canards deflection	η	deg
25	Flap setting	δ_{FL}	deg
76	Flight path angle	θ	deg
77	Indicated airspeed	V_{IAS}	km/h
63	Left engine throttle setting	δ_{ENG1}	%
35	Longitudinal load factor (body axes)	n_X	-
19	North coordinate	N	m
14	Pitch angle	ϑ	deg
331	Pitch angle (wind axes)	ϑ^W	deg
4	Right aileron deflection	χ	deg
10	Rudder deflection	ζ	deg
37	Side load factor (body axes)	n_Y	-
11	Sideslip angle	β	deg
216	TVC nozzles angle (*XZ* plane)	φ_{TV}	deg
36	Vertical load factor (body axes)	n_Z	-
32	Vertical speed (rate of climb/descent)	V_Z	m/s

OUTPUT FORMATS – The selected 20 flight variables can be recorded using several representation formats. The purpose of these formats is (1) to represent the output information most efficiently, and (2) to facilitate further logical and statistical analysis of flight. In this study, the frequency of flight data recording is 4 Hz. After each experiment, VATES creates a set of output files, coded by a flight identification number. This output can be depicted and analyzed using data and knowledge mapping formats. The *output data formats* include: data tables (up to ten), each containing up to 20 flight variables, plotted time-histories of these variables, and a flight scenario time-history. There is also a special output file, which contains information for a 3-D graphics viewer MAGE [11]. The developed *knowledge mapping formats* include the following diagrams: flight scenario time-history, 3-D flight path profile, 4-D "flight movie", 3-D "flight path–roll ribbon", 3-D "flight path-events", 3-D "flight path–ribbon–events", 2-D and 3-D phase diagrams, situational tree [7], flight safety spectra [7], and some other. The first six formats will be demonstrated below.

SIMULATION EXAMPLES – A "bird-eye" view of the aerobatic sequence simulated according to scenario **S** is shown in **Fig. 2**. This diagram is called a 4-D *"flight movie*". This is basically a sequence of multiple snapshots of the vehicle linear and angular position in air space from 1^{st} to 415^{th} second. The time interval between two adjacent snapshots is one second. Also shown here are three axes of the earth coordinate system. Note that the runway's front end is located at (0,0,0). A 3-D *"flight path–roll ribbon"* diagram of this display sequence is depicted in **Fig. 3**. Its directional cosine matrix is the same as in **Fig. 2**. The meaning of the flight "ribbon" concept is clear from the diagram. The numbers 1, …, 32 on the diagram correspond to the flight breakdown into segments (**Table 2**). A *flight scenario time history* is presented in **Table A3** and **Fig. 4**. This example corresponds to segments 11-16. Time histories of the selected 20 output variables are depicted in **Fig. A1**. Valuable information is also presented in **Fig. 5**, which is called a *3-D "flight path-events" diagram*. This is the calendar of all recognized events $\mathbf{E}_i$, shown attached to the flight path at time instants $t(\mathbf{E}_i)$. The numbers at the flight path indicate the start and end points of segments $S_{1\text{-}2}$, …, $S_{31\text{-}32}$. All ten phases of flight $P_{(1)}$, …, $P_{(10)}$ are shown separately in **Fig. 6-23** in the "movie" format. Note that the size of the depicted vehicle is not proportional to the flight path geometry. Brief explanations for these figures are summarized in **Table 8**.

HYPOTHETICAL MANEUVERS – A broad range of hypothetical maneuvers has been generated using autonomous modeling and simulation. **Fig. A2-A14** represent a small series of examples of such maneuvers, both safe and unsafe. Reference numbers and brief explanation of these figures are provided in **Table 9**. The words "unsafe", "marginal" and "safe" are used to characterize the overall safety status of each maneuver. A brief discussion of the simulated cases will follow - ref. **Tables 8-9** and **Fig. 2-23**, **A1-A14**.

Table 8. List of figures containing 4-D "movies" for phases $P_{(1)}$, …, $P_{(10)}$

Fig.	Phase	Content
6	(1)	Takeoff, vertical climb, 180° right roll, and ¾ loop (general view)
7	(2)	First Pougatchev Cobra (general view)
8		Cobra fragment (side view)
9	(3)	Left turn, 270° heading change, ¼ loop (general view)
10	(4)	Vertical climb and vertical descent with multiple rolls (general view)
11		Upper part of the maneuver (side view)
12	(5)	Loop, vertical climb; descent from a fixed 90° pitch vertical position (general view)
13		Loop (fragment, side view)
14		Sharp change of flight path (fragment, side view)
15		Sharp change of flight path (fragment, top view)
16	(6)	Right turn for heading reversal; second Cobra maneuver (general view)
17		Cobra maneuver (fragment, side view)
18	(7)	Loop with 90° roll, followed by a loop with a single Somersault and descent at medium pitch (side view)
19	(8)	Vertical climb, sharp dive using TVC, double Somersault and tail-down slide (general view)
20		Double Somersault and tail-down slide (side view)
21		Sharp path bending (fragment, side view)
22	(9)	S-turn to gain the runway heading (0°) – general view
23	(10)	Landing approach, landing, touchdown, and groundroll (general view)

DISCUSSION

Note. The presented series of maneuvers is not systematic. The primary purpose of these examples is to test and demonstrate capabilities of autonomous modeling and simulation in studying complex aerobatic domains. Each of these maneuver patterns can and should be explored further (e.g.: to assess its sensitivity to structural and parametric variations in piloting tactics and nonstandard flight conditions). For example, "safety cones" of allowed input and output conditions are to be derived for each key scenario component. All findings relate to a notional highly maneuverable vehicle.

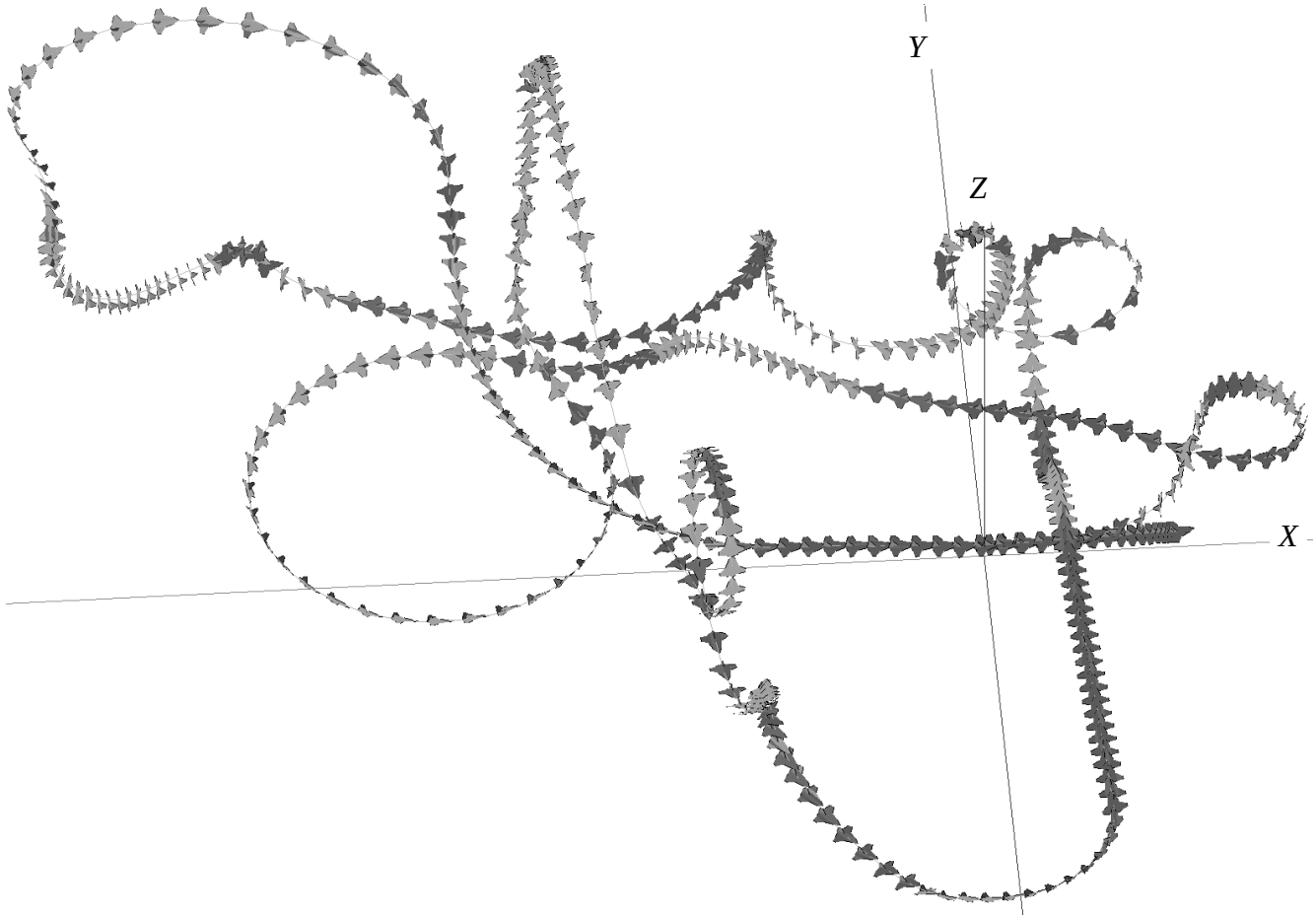

Fig. 2. Simulated aerobatic flight sequence

Table 9. A list of figures containing hypothetical maneuvers

Fig.	Content
A2	Vertical climb with TVC; the vehicle is "frozen" at a top point (at about zero airspeed), then stalled (unsafe)
A3	A nozzles-up Somersault in ascending flight and a tail-down descent (both under TVC); left wing slide and escape (marginal)
A4	Nozzles-up Somersault in ascent, short but deep left-wing sideslip and tail-down descent under TVC (safe)
A5	Takeoff, vertical climb, ¾ loop with a slow nozzles-up double Somersault, and a medium-pitch descent for landing under TVC (marginal)
A6	This is a variation of the scenario shown in **Fig. A5**: the Somersault is performed faster, thus with more time left to level the vehicle and restore its energy balance for landing or go-around under TVC (safe)
A7	Takeoff, vertical climb, ½ loop with a slow ½ Somersault, and a tail-down (90° pitch) descent under TVC, e.g.: for vertical "docking" (safe)
A8	Vertical climb, a slow nozzles-down ½ Somersault, vehicle "frozen" position during a tail-forward small pitch descent, finished by a slow nozzles-down ¼ Somersault; note: a fragment of other, irrelevant segment is visible (safe)

Table 9. A list of figures containing hypothetical maneuvers (Continued)

Fig.	Content
A9	A deep Cobra maneuver performed near the ground, recovery at a medium-pitch angle, followed by a fast vertical climb: all elements are due to TVC (safe)
A10	Vertical climb, loss of airspeed, stall, and fast spin (unsafe)
A11	A mirror image of a "flight path-roll ribbon" of the maneuver from **Fig. A10**
A12	Vertical climb, nozzles–up Kulbit; "frozen" medium-pitch tail-first slide, climb, irregular Cobra (with oscillations in roll and sideslip), recovery in climb (marginal)
A13	Takeoff, vertical climb with a 180° roll, followed by a "knife"-like path, which is a result of a coordinated turn in vertical plane; this maneuver requires a special combination of pitch and roll angles measured in wind axes (safe)
A14	Takeoff, loop and 1½ Somersault, descent, Cobra, and a sequence of two up-down maneuvers in vertical plane with sharp changes of the flight path at top points by TVC (safe)

The following issues are briefly discussed below: flight scenario complexity, reference frames, knowledge mapping formats, thrust vectoring, integrated flight control, Cobra, Somersault, and tail slide maneuvers.

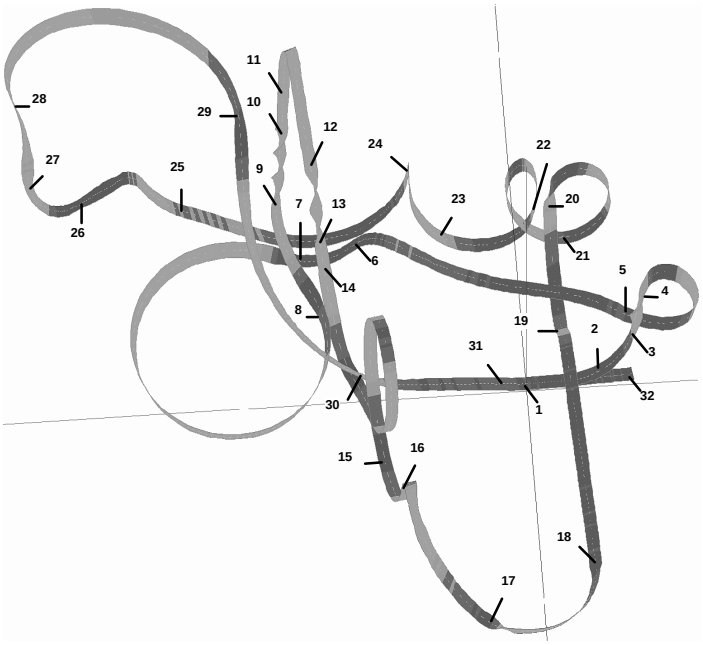

Fig. 3. 3-D flight path–roll ribbon

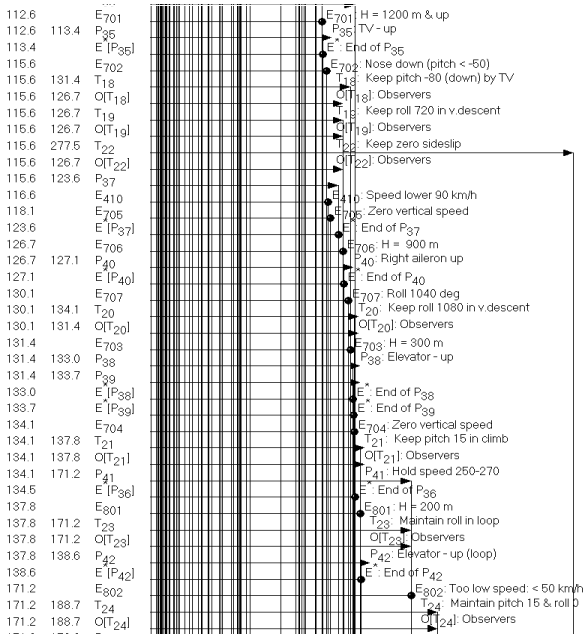

Fig. 4. Flight scenario time history (example)

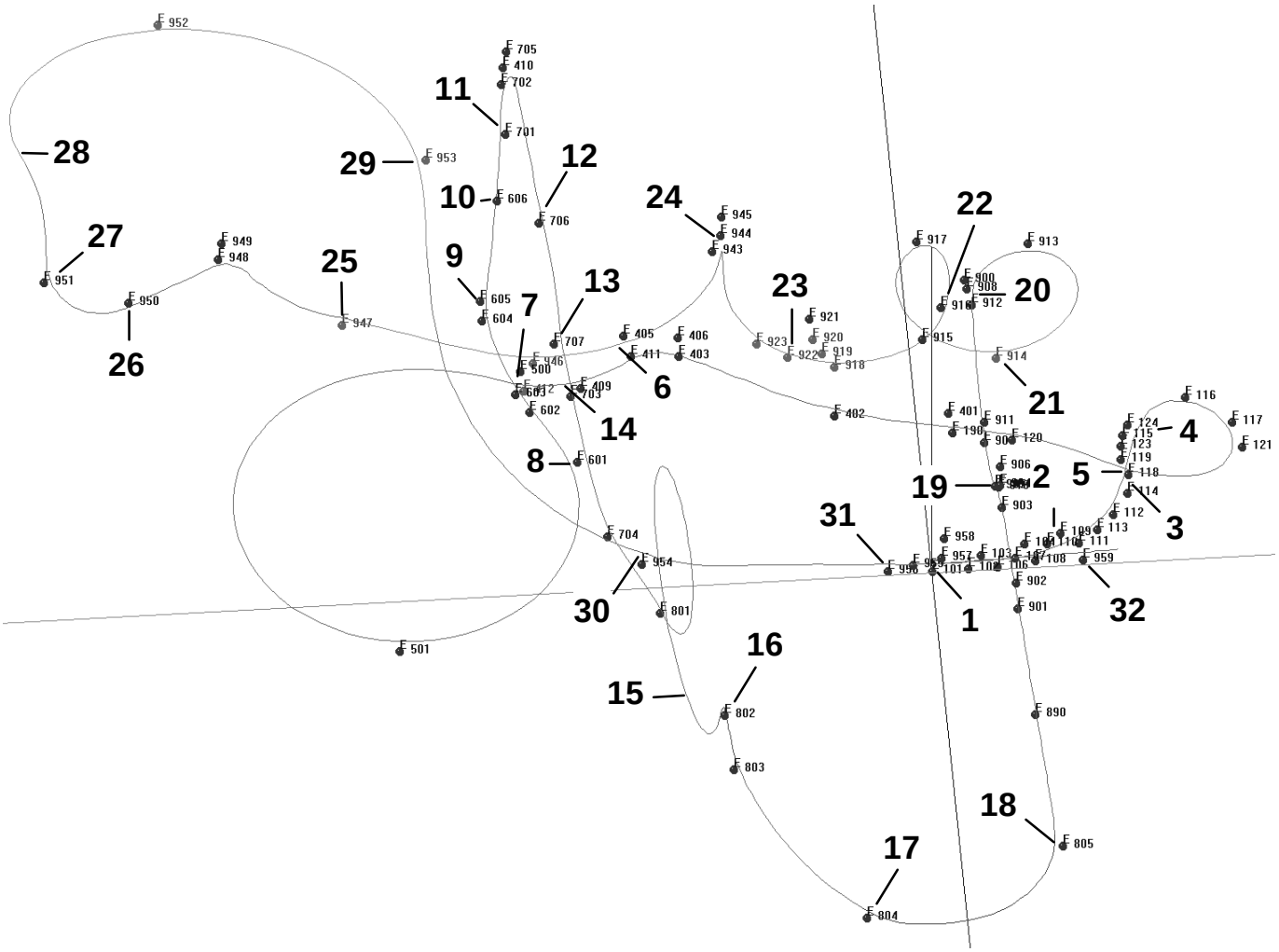

Fig. 5. Flight path - events diagram

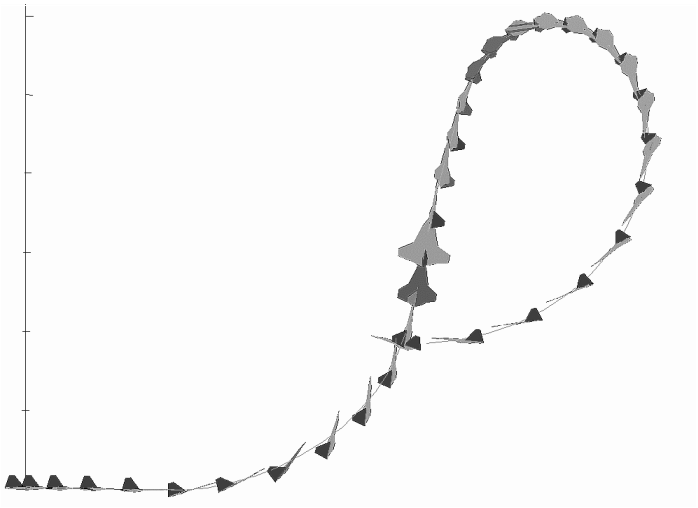

Fig. 6. Takeoff, vertical climb, 180º right roll, and ¾ loop

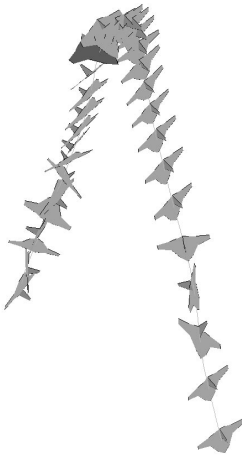

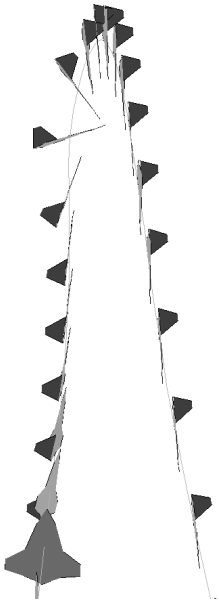

Fig. 10. Vertical climb and vertical descent with multiple rolls

Fig. 11. Upper part of the previous maneuver (side view)

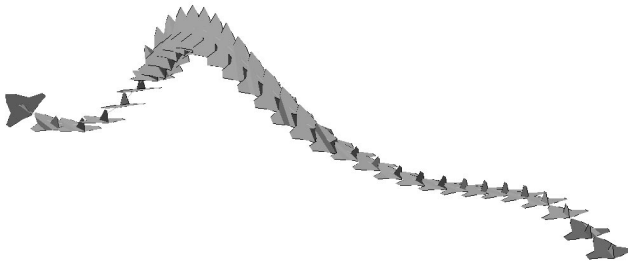

Fig. 7. First Pougatchev Cobra-like maneuver

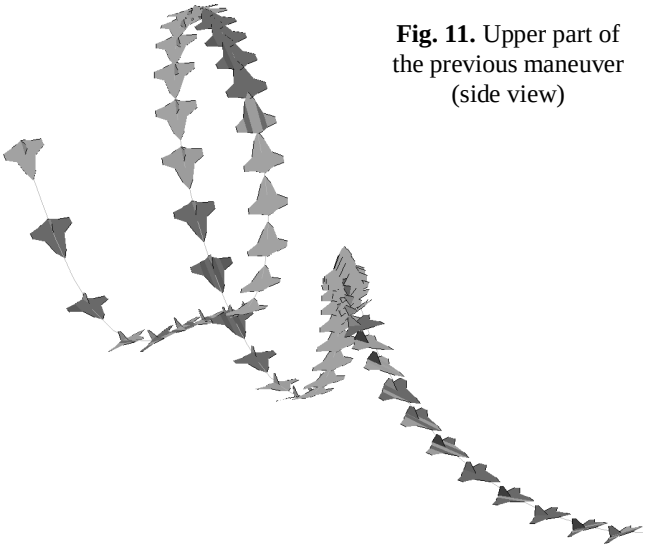

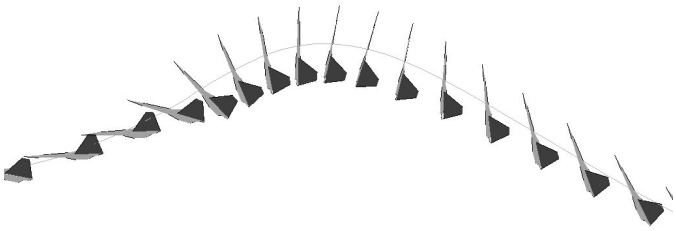

Fig. 8. Cobra fragment (side view)

Fig. 12. Loop, vertical climb; descent from fixed 90º pitch vertical position

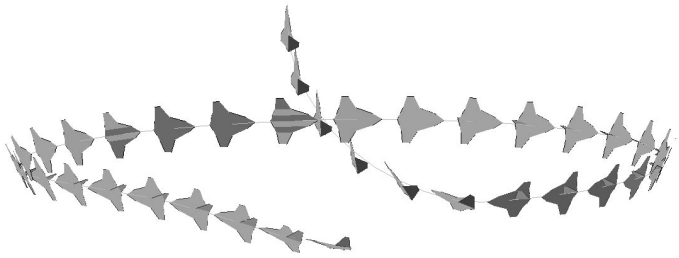

Fig. 9. Left turn, 270º heading change, ¼ loop

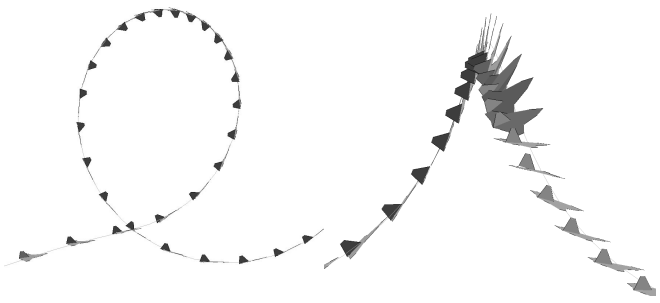

Fig. 13. Loop from **Fig. 12** (side view)

Fig. 14. Sharp change of flight path from **Fig. 12** (side view)

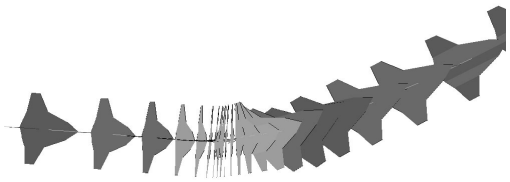

Fig. 15. Sharp change of flight path from **Fig. 12** (top view)

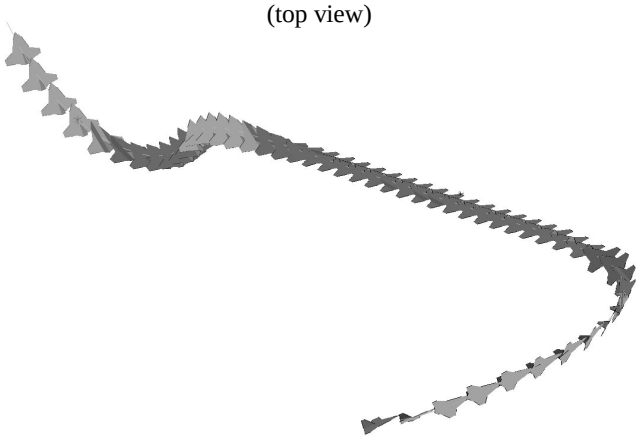

Fig. 16. Right turn for heading reversal; second Cobra maneuver

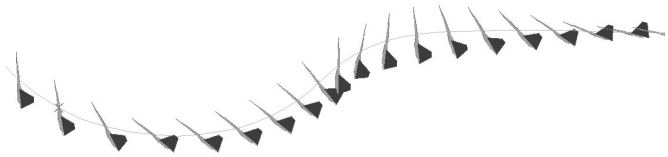

Fig. 17. Second Cobra maneuver (side view)

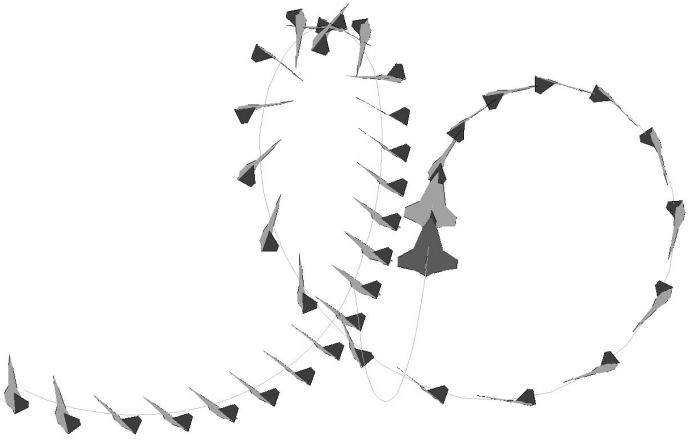

Fig. 18. Loop with 90º roll, followed by a loop with a single Somersault and descent at medium pitch (side view)

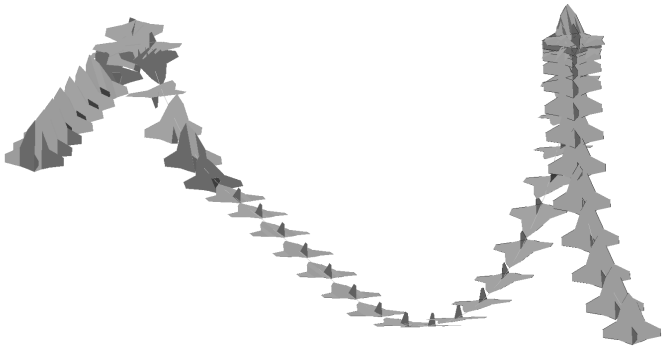

Fig. 19. Vertical climb, sharp dive using TVC, double Somersault and tail-down slide

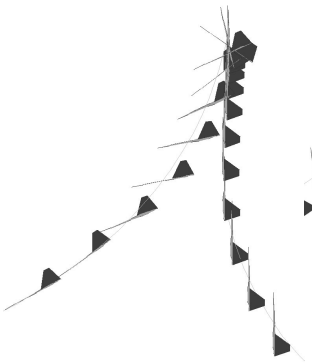

Fig. 21. Sharp path bending (fragment of **Fig. 19**, side view)

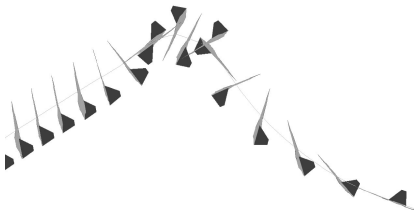

Fig. 20. Double Somersault and tail-down slide (fragment of **Fig. 19**, side view)

Fig. 22. S-turn to gain the runway heading (0º)

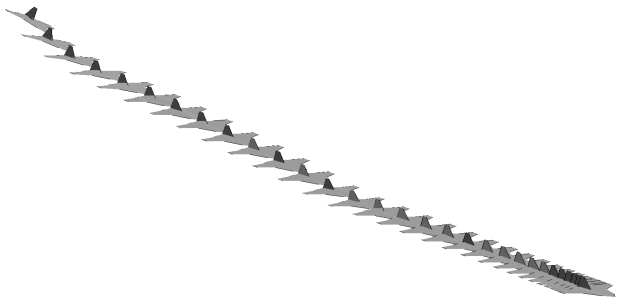

Fig. 23. Landing approach, landing, touchdown, and groundroll

FLIGHT SCENARIO COMPLEXITY – **Fig. A1** demonstrates, in particular, that the examined scenario is a dynamic, realistic and complex sequence. Its complexity is close to and, in some elements, exceeds the level of complexity of the actual scenario (**Fig. 1**). It is essential that autonomous aerobatic simulation, as well as actual aerobatic flying, requires a coherent use of flight controls, careful planning of structure and parameters of a flight scenario.

REFERENCE FRAMES – Careful selection of reference frames for measuring model attitude and defining goal states is essential. It helps design robust sets of the system state observers, which satisfy both the maneuver precision and the flight safety criteria. A more detailed analysis and discussion of this issue is beyond the scope of this paper.

KNOWLEDGE MAPPING FORMATS – Autonomous modeling and simulation combined with computer graphics technologies allow to analyze complex flight domains at a higher level of abstraction and generalization. As a result, complex system relationships can be identified and examined in quantitative and qualitative terms more effectively. In particular, a "flight path–roll ribbon" diagram is a knowledge mapping format, which explicitly shows a dynamic relationship between the aircraft flight path and roll attitude (**Fig. 3**). The density of flight event distribution along the flight path (**Fig. 4**) serves as a measure of flight scenario complexity. Scenario time-history diagrams help formalize the structure and logic of piloting tactics (**Fig. 5**). Several flight complexity measures and knowledge mapping formats of even a higher level can be built on this basis [9].

THRUST VECTORING. INTEGRATED FLIGHT CONTROL – There are several possible modes of thrust vectoring control, including symmetric, asymmetric, and differential vectoring. In this study only symmetric deflections of engine nozzles in the aircraft's normal plane have been tested. Thrust vectoring can be used for designing new maneuvers and enhancing existing ones, as well as a backup flight control method. In particular, the model has demonstrated the TVC capability to "freeze" the vehicle in a required position or rotate it at a required angular velocity at low flight speeds (ref. **Fig. 8**, **11**, **14**, **15**, **17**, **18**, **20**, **21**, **A2**, **A4-A9**, **A12**, and **A14**). However, this observation should be verified in future simulations using vehicle-specific data and in flight tests. TVC helps change the vehicle flight path quickly and thus acquire a safe evasive mode at low and medium flight speeds. Equally, TVC can bring the vehicle abruptly to an unsafe motion mode or attitude, especially if combined with inadequate or deficient yaw and roll control. Combined flight control methods (e.g.: elevator + canards + symmetric TV, ailerons + asymmetric TV) can be explored in realistic operational scenarios using the autonomous model. Also, if vehicle's aerodynamics describes critical flight regimes, some chaotic motion modes can be studied as well.

COBRA MANEUVER – Simulation has demonstrated several possible variations of a classical Pougatchev Cobra maneuver - ref. **Fig. 8**, **17**, **A4**, and **A9**. Some other cases, which are a blend of positive features of Cobra and other figures, have also been tested (not shown). Further research is needed into this spectacular maneuver and its "neighborhood" using more refined vehicle data and flight tests. In particular, input and output safety margins can be identified for this maneuver, its derivative and mixed cases.

SOMERSAULT – Fig. **18**, **21**, **A3**, **A4**-**A7**, **A12** depict some hypothetical examples of the Somersault maneuver. The difference between the original Somersault (**Fig. 1**) and these cases (except for **Fig. A12**) is that the model rotates about its lateral axis without significantly disturbing the loop's curvature. Nozzles-up and nozzles-down and slow and fast rotation versions of this maneuver are possible. Pitch attitude, altitude and airspeed of the vehicle are essential when exiting a Somersault to secure the vehicle's energy balance and flight safety.

TAIL SLIDE – Several patterns of vehicle tail slide, similar to one demonstrated in **Fig. 1**, have been simulated. **Fig. 14-15** depict tail slides under elevator control, and **Fig**. **22**, **A4**, **A7**, and **A8** show examples of the tail slides made under TVC. Tail slides, including hovering or "walk" modes in a vertical position are potentially useful. One of prospective applications of this maneuver, which needs further analysis, is vehicle vertical "docking" or near-vertical (at 60°-80° pitch angles) landing.

CONCLUSION

The developed autonomous modeling and simulation technique is capable of performing fast-time numeric analysis of realistic aerobatic scenarios of highly maneuverable aircraft. Invariant cause-and-effect relationships, which determine the "pilot (automaton) – vehicle – operational environment" system behavior and safety under complex conditions can be identified and measured. This technique enables a systematic exploration of unknown and potentially unsafe flight maneuver domains and reconstruction of aerobatics-related accidents and incidents. Equally, it can serve as a virtual flight test/operation article in applied aerodynamic studies, physics-based pilot training, and in new maneuvers design. However, manned simulations and flight tests are required to validate this technique and verify results of simulation for a given vehicle and maneuvering scenario. Linking, branching and automation of aerobatic maneuvers is another prospective research area.

Finally, the following conclusion relates to the roots of some aerobatics-related flight accidents with highly maneuverable aircraft. Modern aerobatic flight is a very

complex and carefully balanced sequence of marginally safe maneuvers, a product of many probes and errors. Last-minute structural changes to such a scenario should not be allowed. A systematic, “what-if” analysis of possible effects of any change to an integral display sequence should be a mandatory procedure before flying a modified scenario. Such analyses will help identify, foresee and avoid a very rare, but dangerous combination of circumstances (“chain reaction”), which may lead the vehicle irreversibly to an accident or incident.

ACKNOWLEDGMENTS

The use of a 3-D graphics viewer MAGE [11], developed by David C. Richardson and Brent K. Presley from Duke University, is acknowledged with gratitude. The authors wish to thank Alan Phillips from Lancaster University (UK), who created the Programmer’s Editor Pfe [12] used in this study.

REFERENCES

1. Gretchikhine, A., http://aeroweb. lucia.it:80/~agretch/RAP.html
2. Borowski, R.A., “Technical Evaluation Report”, *Proceedings of the AGARD Flight Mechanics Symposium on “Technologies for Highly Manoeuvrable Aircraft”, October, 18-21 1993, Annapolis, Maryland, USA, AGARD CP-548,* March 1994, pp. T1-T11.
3. Garwood, K.R., Hodges, G.S., and Rodgers, H.E., ”Engine Characteristics for Agile Aircraft”, *Proceedings of the AGARD Flight Mechanics Symposium on “Technologies for Highly Manoeuvrable Aircraft”, October, 18-21 1993, Annapolis, Maryland, USA, AGARD CP-548,* March 1994, pp. 3-1 – 3-8
4. Fielding, C., “Design of Integrated Flight and Powerplant Control Systems”, *Proceedings of the AGARD Flight Mechanics Symposium on “Technologies for Highly Manoeuvrable Aircraft”, October, 18-21 1993, Annapolis, Maryland, USA, AGARD CP-548,* March 1994, pp. 4-1 – 4-12
5. Barham, R.W., ”Thrust Vector Aided Maneuvering of the YF-22 Advanced Tactical Fighter Prototype”, *Proceedings of the AGARD Flight Mechanics Symposium on “Technologies for Highly Manoeuvrable Aircraft”, October, 18-21 1993, Annapolis, Maryland, USA, AGARD CP-548,* March 1994, pp. 5-1 – 5-14
6. Burdun, I.Y., and Mavris, D.N., “A Technique for Testing and Evaluation of Aircraft Flight Performance During Early Design Phases” (Paper No. 975541), *World Aviation Congress (WAC’97)*, *October 13-16, 1997, Anaheim CA*, SAE Aerospace - AIAA, 1997, 12 pp.
7. Burdun, I.Y., "The Intelligent Situational Awareness And Forecasting Environment (The S.A.F.E. Concept): A Case Study" (Paper No. 981223), *Proceedings of the SAE Advances in Flight Safety Conference and Exhibition, April 6-8, 1998, Daytona Beach, FL, USA" (P-321)*, AIAA - SAE Aerospace, pp.131-144.
8. Burdun, I.Y., "An AI Situational Pilot Model for Real-Time Applications", *Proceedings of the 20th Congress of the International Council of the Aeronautical Sciences, Sorrento, Napoli, Italy, 8-13 September 1996 (ICAS'96)*, Volume 1, AIAA, 1996, pp. 210-237.
9. Burdun, I.Y., and Parfentyev, O.M., "Fuzzy Situational Tree-Networks for Intelligent Flight Support", *International Journal of Engineering Applications of Artificial Intelligence,* **12** (1999), pp. 523-541
10. Burdun, I.Y., A Method for Accident Reconstruction and Neighborhood Analysis Using an Autonomous Situational Model of Flight and Flight Recorder Data (Paper No. 99ASC-12), *SAE 1999 Advances in Aviation Safety Conference and Exposition, Daytona Beach, FL, April 1999*, SAE, 1999
11. Richardson, D.C., and Presley, B.K., “MAGE Version 5.40”, http:// kinemage.biochem.duke.edu/website/kinhome.htm
12. Phillips, A., “Programmer's File Editor (Pfe)”, http://www.lancs.ac.uk/ people/cpaac/pfe

DEFINITIONS, ACRONYMS, ABBREVIATIONS

$\rightarrow$	State transition
η	Elevator position
ϑ	Pitch angle
Π	Flight process
η	Elevator and canards
χ	Aileron
ζ	Rudder
β	Sideslip
ψ	Yaw angle
ϕ	Bank angle
ϑ	Pitch angle
$\Omega(\Pi)$	Calendar of flight processes
$\Omega(\mathbf{E})$	Calendar of flight events
$\Omega(\mathbf{O})$	Calendar of system state observers
$\Omega(\mathbf{X})$	Vocabulary of all system state (flight) variables
$\beta`$	Sideslip rate
δ_{ABR}	Air brake deflection angle
$\delta_{ENG1/2}$	Engine No. 1/2 throttle position
$\delta_{INT1/2}$	Interceptor No. 1/2 deflection angle
φ_{TV}	Engine nozzle deflection angle in *XZ* body plane
ϑ^{w}	Pitch angle (wind axes)
ϕ^{w}	Roll angle (wind axes)
||	Concatenation operation
6-DOF	Six-degree-of-freedom
ABS	Absolute method of defining a flight goal
AI	Artificial intelligence
C.G.	Center of gravity location on MAC
deg	Degree
E	Flight event
E	East coordinate
$\mathbf{E}^{*}$	Target event

$\mathbf{E}_*$	Source event
G	Interim flight goal
H_{wheels}	Altitude measured at main wheels
$i(\mathbf{E}_*)$	Source event code
$i(\mathbf{E}^*)$	Target event code
K_{LG}	Undercarriage on-off control switch
km/h	Kilometer per hour
m	Meter
m	Requested goal definition method
MAC	Mean aerodynamic chord
MAGE	Simple 3-D graphics visualization tool (freeware, ref. [11])
N	North coordinate
N(Ω(…))	Total number of elements in set Ω(…)
n-D	*n*-dimensional, $n \in \{2, 3, 4\}$
n_X	Longitudinal load factor (body axes)
n_Y	Side load factor (body axes)
n_Z	Normal load factor (body axes)
O	System state observer
P	Control procedure
$P_{(i)}$	*i*-th phase of flight
$\mathbf{p}^{`w}$	Roll acceleration (wind axes)
Pfe	Programmer's Editor Pfe (freeware, ref. [12])
$\mathbf{p}^{w}$	Roll velocity (wind axes)
$\mathbf{q}^{`w}$	Pitch acceleration (wind axes)
$\mathbf{q}^{w}$	Pitch velocity (wind axes)
r`	Yaw acceleration
REL	Relative method of defining a flight goal
S	Flight [situation] scenario
S	Flight segment
s	Second
SL	Sea level
t	Current flight time
T	Piloting task
$t(\mathbf{E}_i)$	Timing of flight event $\mathbf{E}_i$
TV	Thrust vectoring
TVC	Thrust vectoring control
u	Control vector
u	Control variable, $u \in \Omega(\mathbf{X})$
VATES	Virtual Autonomous Test and Evaluation Simulator
V_{IAS}	Indicated airspeed
V_R , VR	Rotation speed
V_z	Vertical speed (earth)
x	Vector of flight variables, $x = (x_1, \ldots, x_k, \ldots, x_p)$
X	Longitudinal axis (in body or earth frames)
x	Flight variable, $x \in \Omega(\mathbf{X})$
Y	Lateral axis (in body or earth frames)
Z	Normal or vertical axis (in body or earth frames)
H	Altitude
α	Angle of attack
δ_{FL}	Flap position

APPENDIX

Table A1—Virtual Autonomous Test and Evaluation Simulator (VATES)

Purpose	Autonomous modeling and simulation of the "pilot (automaton)-vehicle-operational environment" system behavior in complex (multi-factor) flight situations
Vehicle class	Fixed-wing aircraft
Modeled motion modes	6-DOF motion, including ground and airborne phases of flight, aerobatic maneuvers, and non-standard situations
Equations of motion	First-order non-linear ordinary equations of motion, in the form of quaternions (permit all attitude flight simulation)
Numeric integration methods	4^{th} order fixed-step predictor-correctors (four options), 2^{nd} order Euler variable step (one), and 4^{th} order fixed-step Runge-Kutta (one)
Flight simulation speed	Groundroll - 20-30 times faster than real time; airborne modes – 20-50 times faster than real time (on a 450 MHz PC)
Simulated aircraft	22 types in total, including 17 airplanes, two helicopters, one tilt-rotorcraft, and two hypersonic vehicles
Input specification of flight	Airworthiness requirements (FAR, etc.); verbal description of a flight situation to examine; test flight description/ program; flight accident data (for reconstruction); Flight Manual instructions; flight test data (for validation and/or reconstruction) – any one option is sufficient
Modeled phases and regimes of flight	Take-off (normal, aborted and continued); landing (normal, continued, go-around maneuver); climb, descent and landing approach (any profile); en-route flight modes (any profile); groundroll; aerobatic, special, and test maneuvers
Confirmed application areas	- Aircraft virtual flight test and certification - Planning and rehearsal of complex flight test programs - Investigation of flight incidents/accidents - Checking Pilot's Manuals under multi-factor conditions - Exploration of flight envelopes under complex conditions - Research into automatic flight control - Pilot training, aerospace education, PhD research
Modeled operating conditions (factors) of flight	- Normal and demanding flight conditions and attitudes - Vehicle weight, C.G. travel, moments/products of inertia - Mechanical failures (engines, control, undercarriage, etc.) and system logic errors - Piloting tactics and pilot errors (see below for details) - Atmospheric conditions (air density and pressure) - Wind (any 3-D profile: gusts, crosswind, microburst, etc.) - Air turbulence (two models) - Rain (effects on vehicle aerodynamics) - Wet, dry, water-covered runway condition, dynamic and uneven surface - Any required combinations of the these factors

Table A1—Virtual Autonomous Test and Evaluation Simulator (VATES) (Continued)

Solved problems	Over 40 applied tasks
Vehicle input characteristics	- Fully loadable (generalized input data format) - 1-, 2-, and 3-dimensional lookup characteristics-tables - Up to 500 input characteristics
Type of flight situation model	Discrete-continuous pilot model; up to 100 events and 200 processes per scenario; any combination of flight dynamics, flight control and demanding operating conditions, including pilot errors, mechanical failures, weather, etc.
Type of built-in "silicon pilot" model	Discrete-continuous multi-step situational (tactical) decision making at three levels: (1) scenario-based flight situation planning contour; (2) situational control contour using "piloting tasks", "system state observers", and "control procedures"; system state observation model includes: observed state variables, gains, goals, errors, insensitivity of state observations, and some other parameters, and (3) automatic response (stimulus-response) control contour
Time to develop a scenario from "scratch"	- 20-30 minutes - Complexity of scenario planning task does not increase with the complexity of a situation under study
Examined scenarios	Over 350 different flight scenario types
Dimension of output state vector	300-500 flight variables describing the "pilot (automaton) – vehicle – operational environment" system behavior
Output data and knowledge visualization formats	- Flight time history tables (up to 20 variables per table) - Flight time history plots (up to 20 variables per plot) - Flight scenario time history listing - Flight experiment statistics - Flight scenario time history diagram - 2-D/3-D phase diagram - 2-D/3-D flight path profile - 4-D "flight movie" diagram - 3-D "flight path-roll ribbon" diagram - 3-D "flight path-events" diagram - 3-D "flight path-roll ribbon-events" diagram - Situational tree diagram - Flight safety/operational effectiveness spectrum - Flight situation complexity diagrams - Multiple constraints violation dynamics/logic diagram
Equipment and user qualification	PC; programming and piloting skills are not required; manned flight simulator is not required; general knowledge of flight dynamics and flight control principles is required

Table A2—Calendar of flight events of aerobatic scenario **S**

$t(E_i)$, *s*	$i(E_i)$	Name
0.1	101	"Groundroll start ..."
4.0	102	"Speed VR achieved"
4.7	103	"Nose wheel off runway"
5.5	105	"Left wheel off runway"
5.5	106	"Right wheel off runway"
6.2	107	"Lift off point"
6.5	104	"Pitch 20 deg"
7.0	108	"H to retract wheels"
7.4	110	"Pitch 30 deg
7.9	109	"Altitude 30 m
8.6	111	"Pitch 60 deg"
9.6	113	"H = 100 m"
10.6	112	"Vertical attitude
12.1	114	"Start of aileron step"
15.0	123	"Roll 135 deg & pitch 90"
15.8	115	"Roll 180 deg & pitch 90"
16.9	124	"Start of 3/4 loop"
22.2	116	"Max altitude (1/4 loop)"
25.4	117	"Nose down (2/4 loop)
27.3	121	"Speed exceeds 250 km/h"
33.0	118	"Nose level (3/4 loop)"
33.3	119	"Zero vertical speed"
37.5	120	"Time 37.5 sec"
40.1	190	"Time 40 sec"
40.3	401	"Time 40.2 sec"
45.0	402	"Time to start Cobra"
53.1	403	"Pitch 85 deg & up"
53.2	406	"Load factor < 1.0"
57.5	411	"Vertical speed < -20 m/s"
58.5	405	"Pitch 55 deg & down"
62.8	409	"Speed exceeds 250 km/h"
65.1	412	"Time 65 sec"
65.2	500	"Time 65 sec"
85.1	501	"Time 85 sec"
95.1	601	"Time 95 sec"
97.1	602	"Time 97 sec"
97.7	603	"Pitch 60 deg & up"
100.5	604	"Pitch 90 deg (vertical)"
101.4	605	"H = 450 m"
108.4	606	"Roll 680 deg & pitch 90 deg"
112.6	701	"H = 1200 m & up"
115.6	702	"Nose down (pitch < -50 deg)"
116.6	410	"Speed lower 90 km/h"
118.1	705	"Zero vertical speed"
126.7	706	"H = 900 m"
130.1	707	"Roll 1040 deg"
131.4	703	"H = 300 m"

Table A2—Calendar of flight events of aerobatic scenario **S** (Continued)

$t(E_i)$, *s*	$i(E_i)$	Name
134.1	704	"Zero vertical speed"
137.8	801	"H = 200 m"
171.2	802	"Too low speed < 50 km/h"
180.3	803	"Speed 170 km/h & up"
188.7	804	"Positive vertical speed"
200.4	805	"H to make pre-Cobra path"
210.1	890	"Time 210 sec"
218.1	901	"Time 218 sec"
219.1	902	"Phase 9 start + 1 sec"
225.1	903	"Pitch 75 deg"
225.8	904	"Pitch > 90 deg"
225.8	906	"Load factor < 1.0"
227.0	910	"Steep descent < -15 m/s"
229.3	905	"Pitch < 55 deg"
234.8	909	"Speed exceeds 250 km/h"
234.8	911	"Vertical speed +5 m/s"
240.4	912	"H to start dual loop"
241.3	908	"H to roll 90 deg"
242.1	900	"Roll 1180 deg"
245.5	913	"First max altitude"
251.8	914	"First min altitude"
253.9	915	"Pitch 70 deg"
261.8	917	"Second maximum altitude"
269.0	916	"H to add thrust"
277.5	918	"Second min altitude"
278.0	919	"Vertical speed > +5 m/s"
278.3	920	"Vertical speed > +10 m/s"
278.4	921	"Pitch 60 deg"
279.3	922	"Pitch 80 deg (~vertical)"
280.9	923	"H to reduce thrust"
291.4	943	"Vertical rate < +5 m/s"
294.2	944	"Negative pitch < 0 deg"
294.3	945	"Negative vertical rate"
306.1	946	"Positive vertical rate"
313.0	947	"H to start Somersault"
323.0	948	"Pitch 3090 deg: 2 Somersaults"
323.2	949	"Negative vertical rate"
330.6	950	"Altitude to boost power"
340.0	951	"H to gain evasive pitch"
356.9	952	"Minimum east distance"
365.1	953	"Maximum north distance"
385.3	954	"On runway heading"
396.5	956	"Altitude to flare"
397.7	955	"H to idle thrust"
399.1	957	"Main wheels contact"
399.3	958	"Nose wheel contact"
408.4	959	"Ground speed < 100 km/h"

Table A3. Flight scenario time history (example, phase $P_{(1)}$)

```
VATES - Virtual Autonomous Test and Evaluation Simulator.
Proprietary Software. Version 7.1.
Copyright (c) 1984-2000 by Ivan Burdun. All Rights Reserved.
-------------------------------------------------
Flight N 1906:  "Virtual aerobatic flight test"   23/01/2000   13:17:04    VAA-1
-------------------------------------------------
time  ===>     .10 sec.
EVEREC: Flight event #  101 "Groundroll start ...    " is recognized.
        height   ...      2.29 m          V_IAS    ...      9.93 km/h
        vert*    ...      -.10 m/s        path     ...     -1.45 deg
.................................................
        time  ===>     .10 sec
PILOT:  Start of piloting task #  1 " Steer runway centerline        "
        Control vector:    10 (rudder  )
        State observers:  143 (sideslp*)
                          150 (r*_b    )
                           11 (sideslip)
.................................................
        time  ===>    4.01 sec.
EVEREC: Flight event #  102 "Speed VR achieved       " is recognized.
        height   ...      2.40 m          V_IAS    ...    184.74 km/h
        vert*    ...       .07 m/s        path     ...       .06 deg
.................................................
        time  ===>    4.01 sec
PROCON: Start of control procedure  1 "Elevator - up       " (ABS) in   .00 s
        Control vector:      3
                          Elevator
                            5.000
.................................................
        time  ===>    4.66 sec.
EVEREC: Flight event #  103 "Nose wheel off runway   " is recognized.
        V_IAS    ...    207.59 km/h       height   ...      2.43 m
        pitch    ...       .07 deg        bank     ...       .00 deg
.................................................
        time  ===>    4.66 sec
PILOT:  End of piloting task   1 (" Steer runway centerline        ")
        due to the recognition of target event # 103
.................................................
        time  ===>    5.38 sec
PROCON: End of control procedure  1 "Elevator - up       "
        Control vector:      3
                          Elevator
                          -12.000
.................................................
        time  ===>    5.38 sec.
EVEREC: Flight event #  105 "Left wheel off runway   " is recognized.
        V_IAS    ...    231.73 km/h       height   ...      2.58 m
        pitch    ...      3.93 deg        bank     ...       .00 deg
.................................................
        time  ===>    5.47 sec.
EVEREC: Flight event #  106 "Right wheel off runway  " is recognized.
        V_IAS    ...    234.40 km/h       height   ...      2.61 m
        pitch    ...      4.92 deg        bank     ...       .00 deg
.................................................
        time  ===>    6.19 sec.
EVEREC: Flight event #  107 "Lift off point          " is recognized.
        height   ...      4.86 m          V_IAS    ...    253.93 km/h
        vert*    ...      6.84 m/s        pitch    ...     16.71 deg
.................................................
        time  ===>    6.55 sec.
EVEREC: Flight event #  104 "Pitch 20 deg            " is recognized.
        V_IAS    ...    261.05 km/h       height   ...      8.17 m
        pitch    ...     21.68 deg        bank     ...       .00 deg
.................................................
        time  ===>    6.55 sec
PILOT:  Start of piloting task #  2 " Keep pitch 30 initial climb    "
        Control vector:     3 (elevator)    4 (aileron )   10 (rudder  )
        State observers:  324 (pitch*_w)  323 (roll*_w )  143 (sideslp*)
                          151 (q*_b    )  149 (p*_b    )  150 (r*_b    )
                          331 (pitch_w )  330 (roll_w  )   11 (sideslip)
.................................................
        time  ===>    6.97 sec.
EVEREC: Flight event #  108 "H to retract wheels     " is recognized.
        height   ...     14.59 m          V_IAS    ...    267.62 km/h
        vert*    ...     18.30 m/s        pitch    ...     26.34 deg
.................................................
        time  ===>    6.97 sec
PROCON: Start of control procedure  2 "Wheels - up          " (ABS) in    .00 s
        Control vector:     89
                          K_gear
                           1.000
.................................................
        time  ===>    7.43 sec.
EVEREC: Flight event #  110 "Pitch 30 deg            " is recognized.
        height   ...     24.46 m          V_IAS    ...    273.18 km/h
        vert*    ...     25.27 m/s        pitch    ...     31.81 deg
.................................................
        time  ===>    7.93 sec.
EVEREC: Flight event #  109 "Altitude 30 m           " is recognized.
        height   ...     38.95 m          V_IAS    ...    277.04 km/h
        vert*    ...     32.78 m/s        pitch    ...     43.50 deg
.................................................
        time  ===>    7.93 sec
PROCON: Start of control procedure  3 "Elevator+TV - up    " (REL) in    .00 s
        Control vector:    216          3
                          phi_tv    elevator
                         xxx.xxx   -10.809
.................................................
        time  ===>    7.93 sec
PILOT:  End of piloting task   2 (" Keep pitch 30 initial climb    ")
        due to the recognition of target event # 109
.................................................
        time  ===>    7.93 sec
PILOT:  Start of piloting task #  3 " Keep side balance              "
        Control vector:     4 (aileron )   10 (rudder  )
        State observers:  323 (roll*_w )  143 (sideslp*)
                          149 (p*_b    )  150 (r*_b    )
                          330 (roll_w  )   11 (sideslip)
.................................................
        time  ===>    8.58 sec
PROCON: End of control procedure  3 "Elevator+TV - up    "
        Control vector:    216          3
                          phi_tv    elevator
                         xxx.xxx   -20.809
.................................................
        time  ===>    8.65 sec.
EVEREC: Flight event #  111 "Pitch 60 deg            " is recognized.
        height   ...     66.21 m          V_IAS    ...    277.68 km/h
        vert*    ...     42.12 m/s        pitch    ...     63.90 deg
.................................................
        time  ===>    8.65 sec
PILOT:  End of piloting task   3 (" Keep side balance              ")
        due to the recognition of target event # 111
.................................................
        time  ===>    8.65 sec
PILOT:  Start of pilcting task #  4 " Keep vertical path by TV       "
        Control vector:   216 (phi_tv  )    4 (aileron )   10 (rudder  )
        State observers:  331 (pitch_w )  323 (roll*_w )  143 (sideslp*)
                          324 (pitch*_w)  149 (p*_b    )  150 (r*_b    )
                          151 (q*_b    )  330 (roll_w  )   11 (sideslip)
```

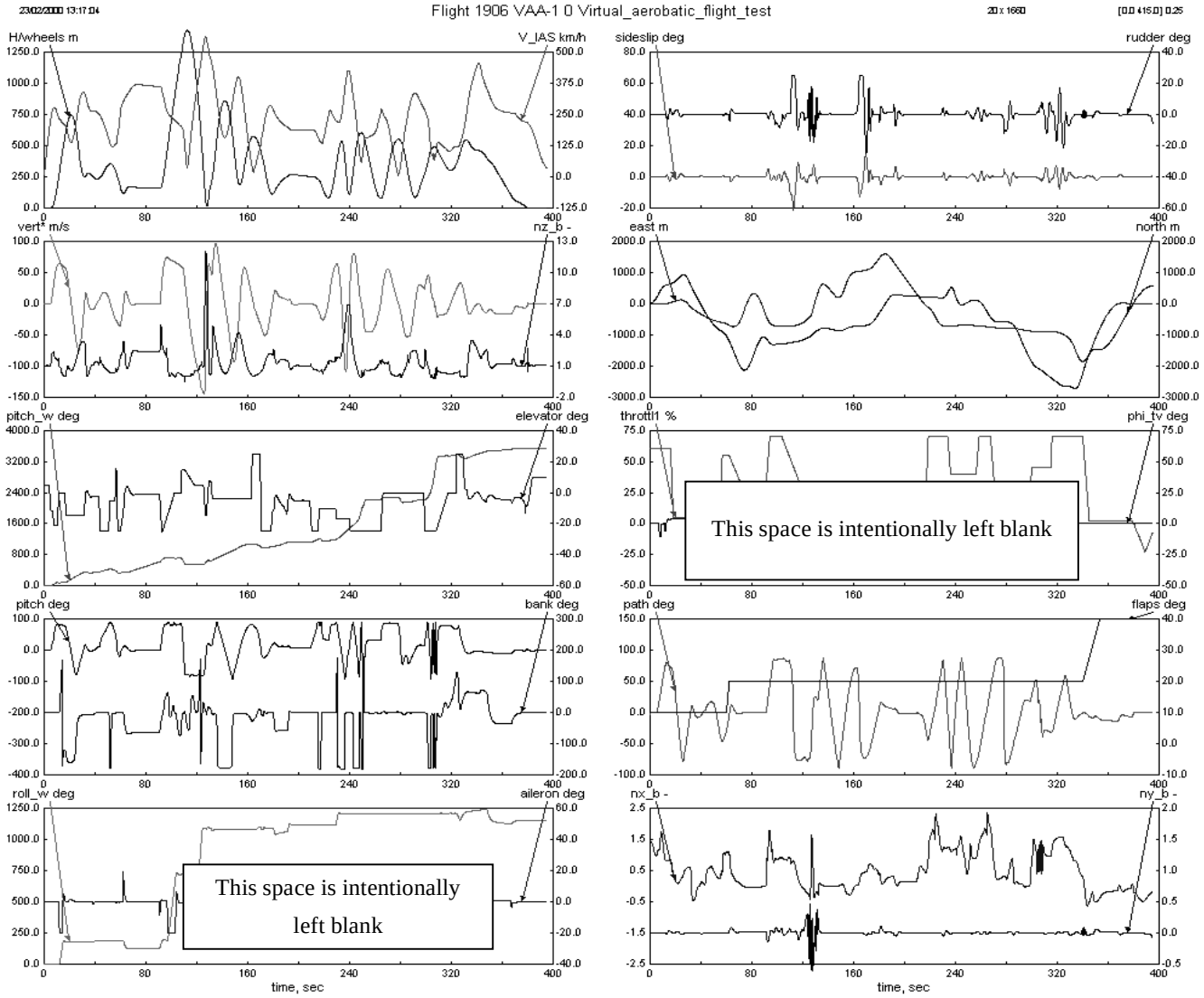

Fig. A1. Aerobatic flight time-history chart (ref. **Table 7**)

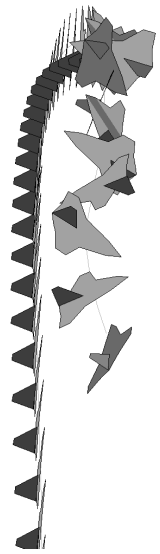

Fig. A2. Flight 1672: vertical climb under TVC; "frozen" position at top at zero speed, then stalled (unsafe)

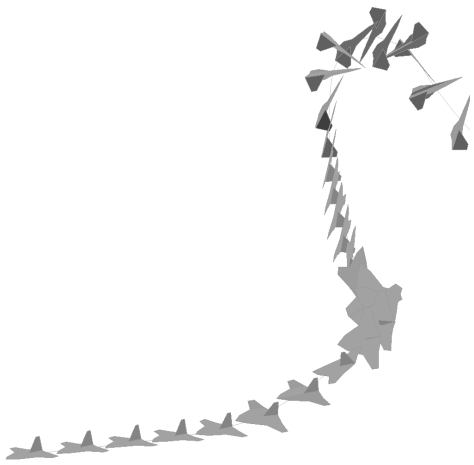

Fig. A3. Flight 1792: nozzles-up Somersault in ascending flight and tail-down descent under TVC; left wing slide and escape (marginal)

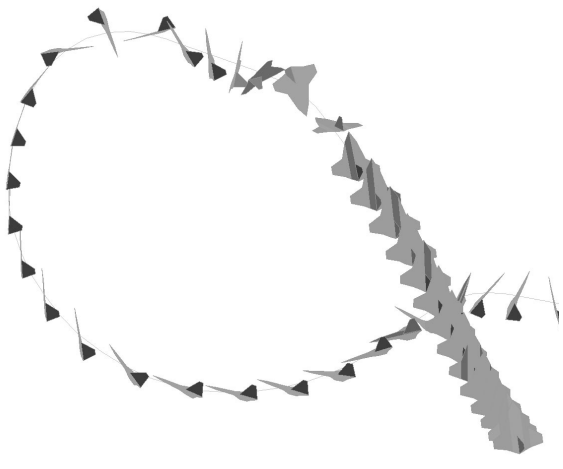

Fig. A4. Flight 1435: nozzles-up Somersault in ascent, short but deep left-wing sideslip and tail-down descent under TVC (safe)

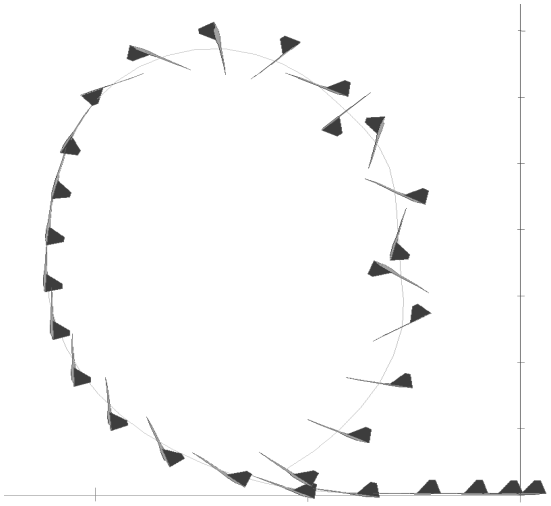

Fig. A5. Flight 942: takeoff, vertical climb, ¾ loop with a slow nozzles-up double Somersault, and a medium-pitch descent for landing under TVC (marginal)

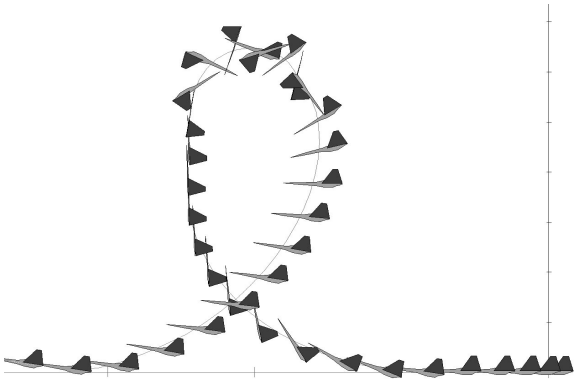

Fig. A6. Flight 804: Variation of **Fig. A5**. Somersault is performed faster, more time is left to level vehicle and restore energy balance for landing or go-around under TVC (safe)

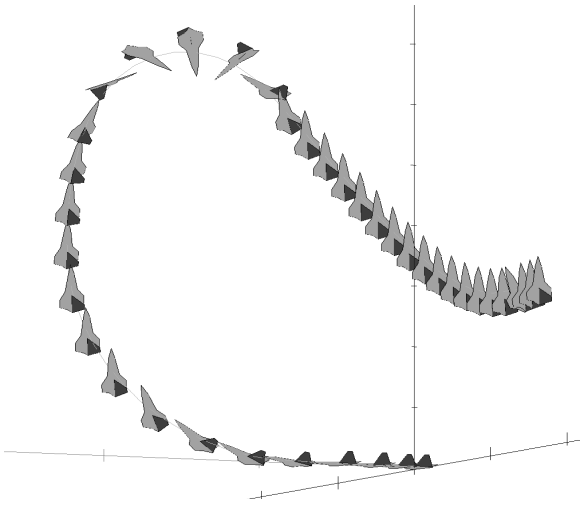

Fig. A7. Flight 950: takeoff, vertical climb, ½ loop with slow ½ Somersault, and tail-down (90^0 pitch) descent under TVC for vertical "docking" (safe)

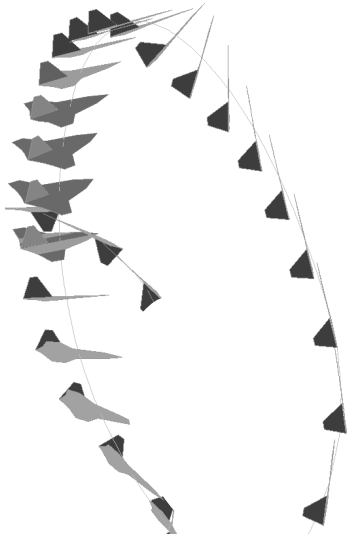

Fig. A8. Vertical climb, a low nozzles-down ½ Somersault, "frozen" position during tail-forward small pitch descent, finished by slow nozzles-down ¼ Somersault (safe)

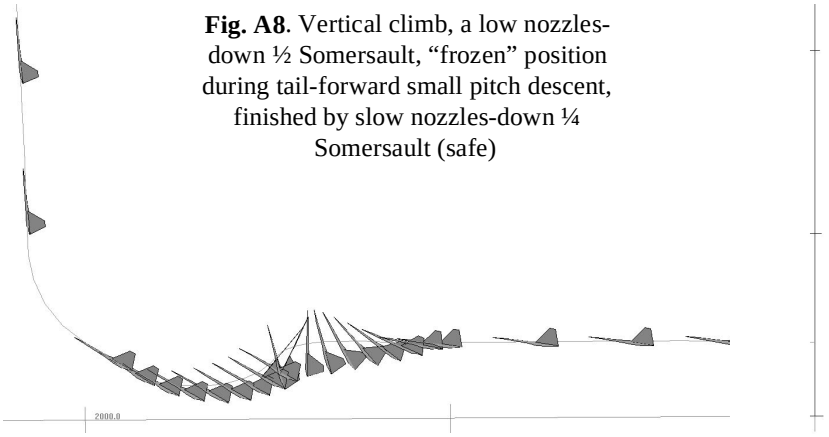

Fig. A9. Deep Cobra performed near the ground, recovery at medium-pitch angle, followed by fast vertical climb. Note: all elements are due to TVC (safe)

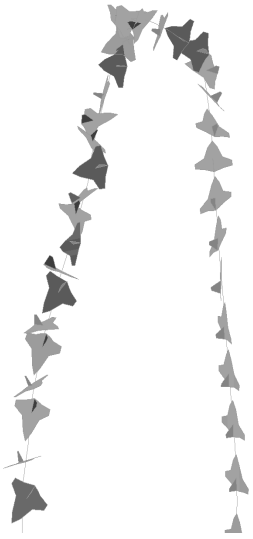

Fig. A10. Vertical climb, loss of airspeed, stall, and fast spin (unsafe)

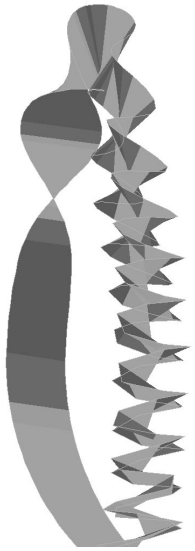

Fig. A11. Mirror image of "flight path-roll ribbon" of maneuver from **Fig. A10**

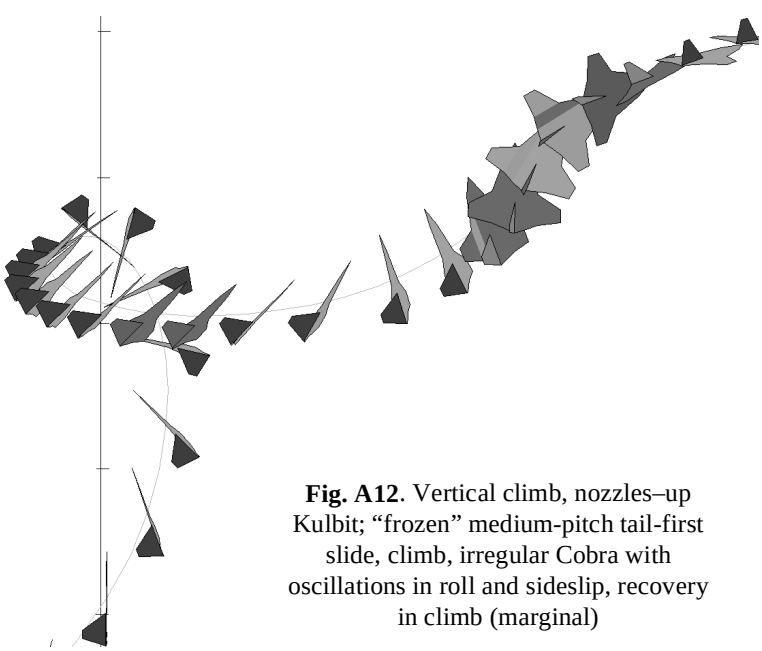

Fig. A12. Vertical climb, nozzles–up Kulbit; “frozen” medium-pitch tail-first slide, climb, irregular Cobra with oscillations in roll and sideslip, recovery in climb (marginal)

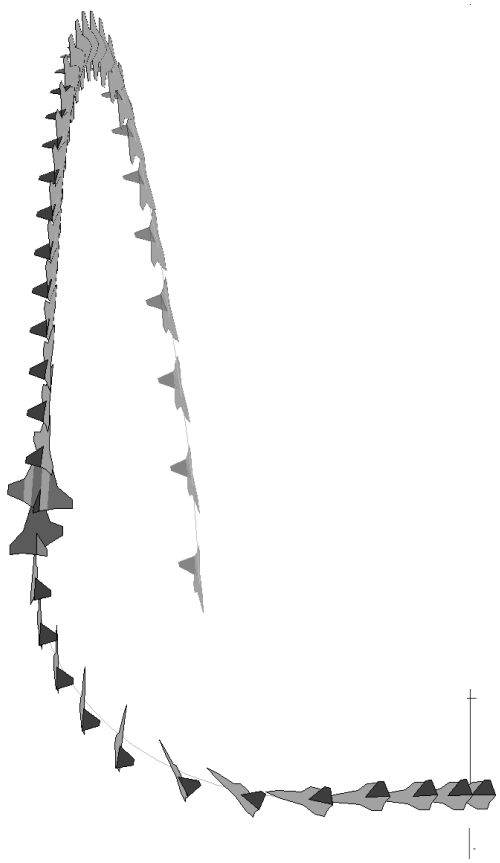

Fig. A13. Flight 1405: takeoff, vertical climb with 180º roll, followed by “knife”-like path; this maneuver requires special combination of pitch and roll angles measured in wind axes (safe)

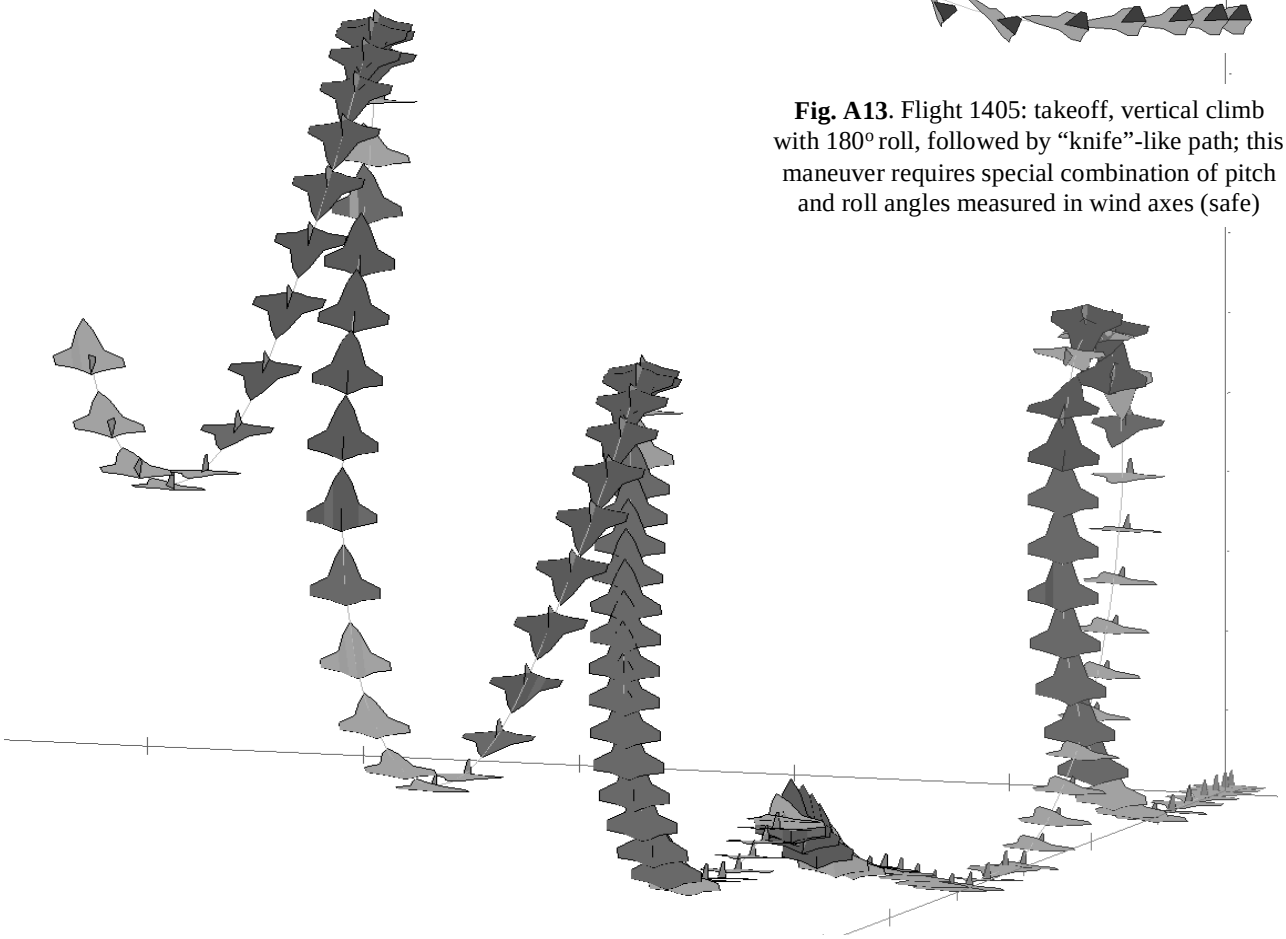

Fig. A14. Flight 940: takeoff, loop and 1½ Somersault, descent, Cobra, and sequence of two up-down maneuvers in vertical plane with sharp changes of flight path at top points by TVC (safe)